Science of the Total Environment 900 (2023) 165844

Contents lists available at ScienceDirect

Science of the Total Environment

journal homepage: www.elsevier.com/locate/scitotenv

# Meteorologically normalised long-term trends of atmospheric ammonia ($NH_3$) in Switzerland/Liechtenstein and the explanatory role of gas-aerosol partitioning

Stuart K. Grange [a,b,*], Jörg Sintermann [c], Christoph Hueglin [a]

[a] Empa, Swiss Federal Laboratories for Materials Science and Technology, Überlandstrasse 129, 8600 Dübendorf, Zürich, Switzerland
[b] Wolfson Atmospheric Chemistry Laboratories, University of York, York YO10 5DD, United Kingdom
[c] Office for Waste, Water, Energy and Air - AWEL, Canton Zürich, Stampfenbachstrasse 12, 8090 Zürich, Switzerland

ARTICLE INFO

Editor: Hai Guo

*Keywords:*
Emissions
Agriculture
Ammonium
Total reduced nitrogen

ABSTRACT

Ammonia ($NH_3$) is an important atmospheric pollutant and despite significant management efforts, trends of $NH_3$ concentrations have not shown progressive decreases over the last few decades across much of Europe. To investigate this issue, long-term $NH_3$ concentrations from passive sampling tubes were analysed at 32 locations across Switzerland and Liechtenstein. A trend analysis controlling for changes in meteorology employing generalised additive models (GAMs) between 2000 and 2021 showed that 29 of the 32 (91 %) sites experienced no significant change or increasing $NH_3$ concentrations with the greatest trend being 0.17 $\mu g\ m^{-3}\ y^{-1}$. These results conflict with an indicated 13 % reduction in $NH_3$ emissions from the Swiss emission inventory. The sensitivity of the $NH_3$ -ammonium ($NH_4^+$) system to reductions of $NH_3$ 's acidic sinks (mostly in the form of nitric and sulfuric acids) was investigated with thermodynamic equilibrium modelling to explain this disconnect. The simulations indicated that the reductions in $NH_3$ 's acidic sinks resulted in less $NH_4^+$ transformation, thus increasing the $NH_3/NH_x$ ratio and this process has compensated for the reduction in $NH_3$ emissions. The average effect of the sink reductions was an increase of 0.9 $\mu g\ m^{-3}$ in $NH_3$ between 2004 and 2021. Increases in the $NH_3/NH_x$ ratio have likely occurred in many European countries due to reductions of acidic precursor emissions and will have consequences for reactive nitrogen deposition and alter import-export budgets among neighbouring regions and countries.

## 1. Introduction

### 1.1. Background

Ammonia ($NH_3$) is an important component of reduced nitrogen ($NH_x$) and is classed as an atmospheric pollutant due to its ability to drive the eutrophication of terrestrial and aquatic environments that can lead to biodiversity loss (Nair and Yu, 2020). $NH_3$ is also an important particulate matter (PM) precursor (Ansari and Pandis, 1998). $NH_3$ is the only significant base in the atmosphere and this makes it a principal component when considering the neutralisation of acids and related chemical pathways (Finlayson-Pitts and Pitts, 2000; Nair and Yu, 2020). When $NH_3$ is emitted into the atmosphere, it is short-lived (between an hour and a day) and undergoes rapid deposition to surfaces, or experiences a gas-to-solid/liquid phase shift to ammonium ($NH_4^+$) in the presence of nitric and sulfuric acid ($HNO_3$ and $H_2SO_4$) (Hertel et al., 2006; Pinder et al., 2008). The result of these reactions is the formation of ammonium nitrate and ammonium sulfate (or bisulfate). Such nitrate- and sulfate-rich PM that results from this $NH_3$ to $NH_4^+$ conversion process often forms large portions of the secondary PM load in European locations, and therefore, makes $NH_3$ an important PM precursor to control across Europe (Wichink Kruit et al., 2017; Jacobsen et al., 2019; Aksoyoglu et al., 2020).

The main $NH_3$ emission source is the agricultural sector, specifically losses from livestock manure and synthetic, nitrogen-rich fertilisers (Sutton et al., 2013; Nair and Yu, 2020; Van Damme et al., 2021). Although there are efforts to control and manage $NH_3$ emissions from agriculture and reduce activities' emission factors, the efforts to control $NH_3$ have generally not been effective enough to reduce emissions to meet the targets that have been set. This can be contrasted with the

* Corresponding author at: Empa, Swiss Federal Laboratories for Materials Science and Technology, Überlandstrasse 129, 8600 Dübendorf, Zürich, Switzerland.
*E-mail addresses:* stuart.grange@empa.ch, stuart.grange@york.ac.uk (S.K. Grange).

https://doi.org/10.1016/j.scitotenv.2023.165844
Received 6 June 2023; Received in revised form 19 July 2023; Accepted 25 July 2023
Available online 29 July 2023

rather successful control efforts that have been applied to other nitrogen species such as $NO_x$ (oxides of nitrogen) where emission reductions have been achieved for road traffic, domestic combustion, energy production, and other industrial processes (Degraeuwe et al., 2017; Sofia et al., 2020). Even though ambient standards are not yet met at many places, $NO_x$ concentrations in Western Europe have substantially decreased over the last two decades. Sulfur dioxide ($SO_2$) is another gaseous pollutant especially relevant to the atmospheric chemistry of $NH_3$ and the European decreases in ambient $SO_2$ concentrations have been even more striking than those seen for $NO_x$ (Vestreng et al., 2007; European Environment Agency, 2020). In contrast, trends of $NH_3$ concentrations are more variable and some countries observe persistently increasing $NH_3$ trends (van Zanten et al., 2017; Wichink Kruit et al., 2017; Jacobsen et al., 2019; Yao and Zhang, 2019; Nair and Yu, 2020; Van Damme et al., 2021). These features of $NH_3$ and $NH_x$ in general, are making $NH_x$ an increasingly important management priority and is set to be an atmospheric pollutant that remains an issue over the next few decades, even as other reactive nitrogen species continue to decrease (The Royal Society, 2021).

The lack of decrease in $NH_3$ concentrations is apparent in some locations even when modest decreases in emissions have been known to be achieved, thus highlighting a disconnect between emissions and ambient concentrations. This observation has been labelled as the "ammonia gap" (Sutton et al., 2003; Bleeker et al., 2009). Studies in North America (Butler et al., 2016; Schiferl et al., 2016; Yao and Zhang, 2016; Yu et al., 2018), Europe (Sutton et al., 2003; Alebic-Juretic, 2008; Tang et al., 2009; Ferm and Hellsten, 2012; Wichink Kruit et al., 2017; Tang et al., 2018), and other locations (Warner et al., 2017) have investigated or speculated on the importance of reductions in acidic precursor emissions (primarily $NO_x$ and $SO_2$), and the consequential decreasing generation of particle phase $NH_4^+$ and persistence of gas phase $NH_3$ concentrations to explain this disconnect. The change in chemical environment and its influence on $NH_3$ concentrations has been approached by different models, such as GEOS-Chem (Yu et al., 2018) and the Operational Priority Substances (OPS) model (Wichink Kruit et al., 2017). To complement chemical transport modelling studies, this work couples long-term observations and thermodynamic equilibrium modelling together to investigate the sensitivity of the changing chemical environment on ambient $NH_3$ concentrations.

### 1.2. $NH_3$ in Switzerland

$NH_3$ emissions in Switzerland are dominated by the agriculture sector with the 2021 national emission inventory (Federal Office for the Environment, 2021, 2022) indicating 94 % of $NH_3$ emissions are sourced from agricultural activities, mainly from stables and the field-application and storage of slurry and manure. $NH_3$ emissions from the agricultural sector have become an increasing focus in Switzerland and despite significant management efforts (Kupper et al., 2015; Frei, 2021), decreases in $NH_3$ concentrations have been elusive at most measurement locations (Philipp and Locher, 2010; Seitler and Meier, 2022; Häni and Kupper, 2021). The strong influence of local sources on local concentrations and the impact of atmospheric processes on the relationship between emissions and measured $NH_3$ concentrations complicates the comparison of the trends of emissions from bottom-up estimates and measurements of ambient concentrations.

The lack of ambient concentration reductions has been apparent, despite the reported reduction of total $NH_3$ emissions of 13 % between 2000 and 2020 (61.6 to 53.3 kt) (Federal Office for the Environment, 2022b). Concerns around eutrophication of sensitive ecosystems is an issue that authorities continue to address (Bundesamt für Umwelt, 2020), as is the continued reduction of $PM_{10}$ and $PM_{2.5}$ concentrations across Switzerland (Bundesamt für Umwelt, 2022). Because secondary nitrate ($NO_3^-$) and sulfate ($SO_4^{2-}$) make up a significant portion of Switzerland's PM load (Grange et al., 2021), these product's precursors (including $NH_3$) are also a priority to control to enable future compliance to the World Health Organization's (WHO) air quality guideline values (World Health Organization, 2021). Switzerland has one industrial $NH_3$ production facility located in Visp, Valais that is not considered a significant $NH_3$ emission source (Federal Office for the Environment, 2022a).

### 1.3. Objectives

This work has two primary objectives. The first is to conduct a robust trend analysis of $NH_3$ concentrations between 2000 and 2021 using passive sampling observations taken at 30 locations in Switzerland and two locations in Liechtenstein. $NH_3$ concentrations will be exposed to a data analysis technique to reduce the influence of weather and weather-driven changes in emission processes on ambient $NH_3$ concentrations. This approach reduces the year-to-year variability of $NH_3$ and allows the estimation of trends with smaller uncertainties. The second objective is to quantify the effect of changes in atmospheric sinks on the trend of ambient $NH_3$ using thermodynamic equilibrium model simulations – specifically investigating the sensitivity of changes in concentrations of acidic precursors during the analysis period. The latter allows a better understanding of the ambient $NH_3$ observations and trends and can be used to verify bottom-up emission estimates.

## 2. Methods

### 2.1. Data

#### 2.1.1. $NH_3$ sampling locations and methods

Atmospheric $NH_3$ concentrations were measured with passive samplers between August 1999 and December 2021 at 30 locations in Switzerland and two locations in the Principality of Liechtenstein (Fig. 1). The sampling activities did not all commence at the same time and the start dates for each sampling location are shown in Table 1. The majority of sampling locations were located on the Swiss plateau, with a noticeable cluster in the centre of Switzerland in the canton of Lucerne where the Swiss agricultural activities are at their most intense (Bundesamt für Statistik, 2021; Federal Office for the Environment, 2021). However, Sion-Aeroport is located in the Rhône Valley and two sampling locations were also located south of the Alps. A map of Switzerland's geographic regions, also called production areas (Federal Office for the Environment, 2020), can be found in the appendix (Fig. A1).

Three different passive $NH_3$ sampling methods were used throughout the 22 years of sampling: Zürcher samplers (Thöni et al., 2003), Radiello samplers (Radiello, 2021), and Ferm samplers (Ferm and Svanberg, 1998). The majority of samples were taken by the Radiello sampler design, but the later sampling periods (from 2019) exclusively used Ferm samplers. The $NH_3$ sampling duration was variable among the locations, but 63 % of the sampling durations were 14 days, 34 % were 28 days, and 3 % (one site) had a sampling duration of 29 days (Table 1; Fig. A2). The number of samples available for analysis was 11,808 with the number of samples for each site ranging from 181 to 547.

The operation of the passive samplers was conducted by eight different authorities or companies but was managed and overseen by Forschungsstelle für Umweltbeobachtung (FUB) (FUB - Forschungsstelle für Umweltbeobachtung AG, 2022) on behalf of the Swiss Federal Office for the Environment, Swiss cantons, and Liechtenstein. FUB conducted the tubes' analysis and handled the quality control and assurance of the measurement procedures. Notably, intercomparisons of the passive sampling methods have been done to demonstrate consistency among the sampler types, see Seitler and Thöni (2009) and Seitler and Meier (2022, page 63). The move from Zürcher to Radiello samplers was accompanied by 294 co-located measurements from eight monitoring sites and based on these parallel measurements, $NH_3$ concentrations obtained from Zürcher samplers were systematically 10 % lower than those determined by Radiello samplers. Therefore, the observations

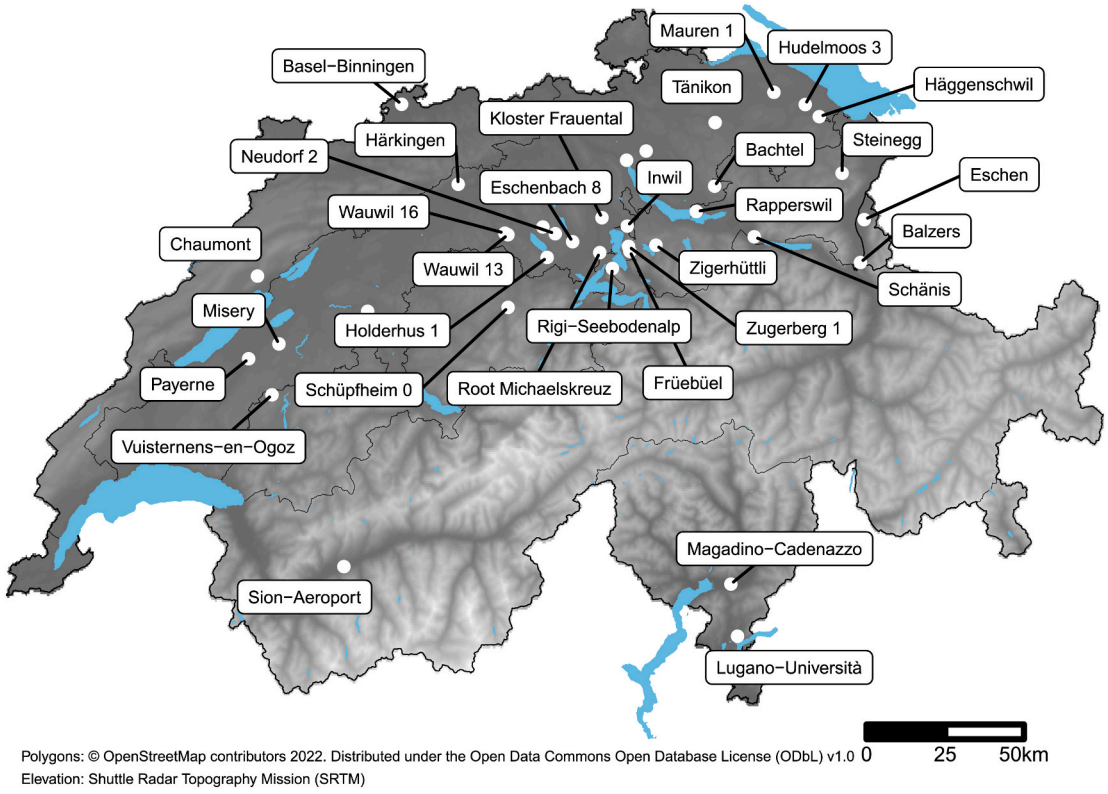


**Fig. 1.** Locations of passive $NH_3$ sampling locations in Switzerland and Liechtenstein between 1999 and 2021. The internal lines show Switzerland's geographic regions and the filled blue areas show larger lakes and reservoirs.

**Table 1**
Information on the 32 $NH_3$ sampling sites in Switzerland and Liechtenstein included in the analysis. The sample duration is the mode and is represented in days. A map of the geographical areas can be found in Fig. A1.

| ID | Country | Site name | Canton | Geographical region | Latitude | Longitude | Elevation (m) | Start date | Sample duration |
|---|---|---|---|---|---|---|---|---|---|
| 1 | CH | Chaumont | Neuchâtel | Jura | 47.05 | 6.98 | 1134 | 1999-09-09 | 14 |
| 2 | CH | Magadino-Cadenazzo | Ticino | Southern Alps | 46.16 | 8.94 | 204 | 1999-09-09 | 14 |
| 3 | CH | Rigi-Seebodenalp | Schwyz | Alps | 47.07 | 8.46 | 1008 | 1999-09-07 | 14 |
| 4 | CH | Schänis | Sankt Gallen | Pre-Alps | 47.15 | 9.06 | 713 | 1999-11-16 | 28 |
| 5 | CH | Payerne | Vaud | Plateau | 46.81 | 6.95 | 488 | 1999-09-09 | 14 |
| 6 | CH | Zugerberg 1 | Zug | Pre-Alps | 47.13 | 8.53 | 950 | 1999-11-02 | 29 |
| 7 | CH | Bachtel | Zürich | Plateau | 47.30 | 8.90 | 907 | 1999-11-01 | 28 |
| 8 | CH | Mauren 1 | Thurgau | Plateau | 47.56 | 9.16 | 439 | 1999-08-31 | 14 |
| 9 | CH | Wauwil 16 | Luzern | Plateau | 47.17 | 8.02 | 495 | 2006-02-02 | 14 |
| 10 | CH | Steinegg | Appenzell Innerrhoden | Pre-Alps | 47.33 | 9.44 | 826 | 2003-02-27 | 28 |
| 11 | CH | Häggenschwil | Sankt Gallen | Plateau | 47.49 | 9.35 | 563 | 2003-02-27 | 28 |
| 12 | CH | Tänikon | Thurgau | Plateau | 47.48 | 8.91 | 535 | 1999-08-31 | 14 |
| 13 | CH | Basel-Binningen | Basel-Landschaft | Jura | 47.54 | 7.58 | 297 | 1999-08-30 | 14 |
| 14 | FL | Balzers | Liechtenstein | Liechtenstein | 47.07 | 9.50 | 472 | 2008-01-08 | 28 |
| 15 | CH | Eschenbach 8 | Luzern | Plateau | 47.15 | 8.30 | 496 | 2004-01-07 | 14 |
| 16 | FL | Eschen | Liechtenstein | Liechtenstein | 47.19 | 9.52 | 437 | 2008-01-08 | 28 |
| 17 | CH | Kloster Frauental | Zug | Plateau | 47.21 | 8.42 | 392 | 2007-01-04 | 28 |
| 18 | CH | Früebüel | Zug | Pre-Alps | 47.12 | 8.54 | 976 | 2007-01-04 | 28 |
| 19 | CH | Härkingen | Solothurn | Plateau | 47.31 | 7.82 | 428 | 2005-04-21 | 14 |
| 20 | CH | Holderhus 1 | Luzern | Plateau | 47.10 | 8.19 | 586 | 1999-11-08 | 14 |
| 21 | CH | Hudelmoos 3 | Thurgau | Plateau | 47.53 | 9.29 | 523 | 2001-01-18 | 28 |
| 22 | CH | Inwil | Zug | Plateau | 47.19 | 8.53 | 439 | 2007-01-04 | 28 |
| 23 | CH | Lugano-Università | Ticino | Southern Alps | 46.01 | 8.96 | 289 | 1999-09-09 | 14 |
| 24 | CH | Misery | Fribourg | Plateau | 46.86 | 7.07 | 594 | 2007-08-10 | 14 |
| 25 | CH | Neudorf 2 | Luzern | Plateau | 47.17 | 8.23 | 745 | 2006-01-31 | 14 |
| 26 | CH | Rapperswil | Sankt Gallen | Pre-Alps | 47.23 | 8.82 | 414 | 2002-12-12 | 14 |
| 27 | CH | Root Michaelskreuz | Luzern | Plateau | 47.11 | 8.41 | 757 | 2001-01-26 | 14 |
| 28 | CH | Schüpfheim 0 | Luzern | Pre-Alps | 46.96 | 8.03 | 718 | 1999-09-15 | 14 |
| 29 | CH | Sion-Aeroport | Valais | Alps | 46.22 | 7.34 | 480 | 1999-09-08 | 14 |
| 30 | CH | Vuisternens-en-Ogoz | Fribourg | Pre-Alps | 46.71 | 7.04 | 831 | 2005-12-15 | 14 |
| 31 | CH | Wauwil 13 | Luzern | Plateau | 47.17 | 8.03 | 497 | 2004-01-07 | 14 |
| 32 | CH | Zigerhüttli | Zug | Pre-Alps | 47.13 | 8.65 | 974 | 2007-01-04 | 28 |

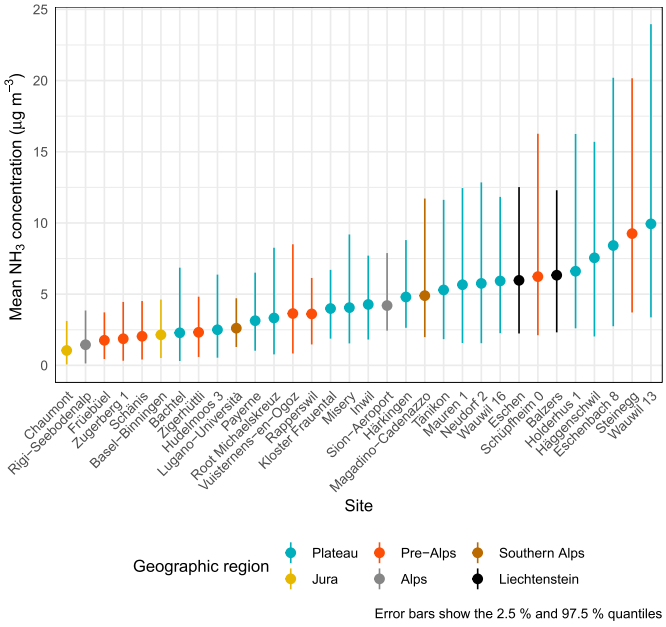


**Fig. 2.** Mean $NH_3$ concentrations with quantiles for 32 passive sampler locations with a sample duration between two and four weeks in Switzerland and Liechtenstein between 2000 and 2021.

from Zürcher samplers between 2000 and 2003 were corrected with a 1.1 multiplier (Seitler and Thöni, 2009). Parallel measurements between Radiello and Ferm samplers have occurred since 2009 and no systematic differences between these two methods have been found, therefore, no data correction was applied when the Radiello samplers were replaced by Ferm passive samplers in 2019. Other measurement techniques, notably mini denuders (discussed below) have also been used as part of the quality control process.

### 2.1.2. Supplementary measurements

Between 2007 and 2021 at three locations, Rigi-Seebodenalp, Payerne, and Magadino-Cadenazzo (Fig. 1; Table 1), $NH_x$ sampling was conducted with mini denuder samplers as part of the NABEL monitoring network's extended operations. Full details of the instrumentation and analysis procedure can be found in Empa (EMPA, 2020, Section 3.12.3), but the use of mini denuders allowed for $NH_x$, $NH_3$, $NH_4^+$, $HNO_3$, and $NO_3^-$ to be quantified every two-weeks in three locations that represent three of Switzerland's geographical regions (Fig. 1; Fig. A1). Daily impregnated filter sampling and analysis methods also quantified $NH_x$ and total $NO_3^-$ at Rigi-Seebodenalp and Payerne between 2000 and 2021, again as part of NABEL's ancillary operations Empa (EMPA, 2020, Section 3.12.2). Particulate sulfur measurements at Payerne, Rigi-Seebodenalp, and Lugano-Università were also used in the analysis. The sulfur measurements were transformed into $SO_4^{2-}$ by assuming all sulfur was in the form of $SO_4^{2-}$. Finally, daily observations of so-called "crustal elements" – sodium, chloride, calcium, potassium, and magnesium for Payerne and Magadino-Cadenazzo were sourced from an intensive PM sampling campaign where samples were taken between 2018 and 2019 (Hüglin and Grange, 2021; Grange et al., 2021, 2022).

The use of these supplementary measurements was required for some simulations and exactly what species and data sets were used is explained fully in Section 2.2.2. The mini denuder and impregnated filter observations were prepared and were exposed to the same analysis method used for the $NH_3$ passive sampling tube observations that controlled for changes in meteorology over time (Section 2.2.1).

### 2.1.3. Meteorological data

The analysis of $NH_3$ observations required access to meteorological data. The data source used for meteorology was the ERA5 reanalysis fields (Copernicus Climate Change Service (C3S), 2017) that have spatial resolutions of 0.25 × 0.25 decimal degrees (in Switzerland, this is approximately equal to 19 × 28 km) and a temporal resolution of one hour. The use of the ERA5 reanalysis fields required pre-processing to be matched with the $NH_3$ observations. The steps included: the extraction

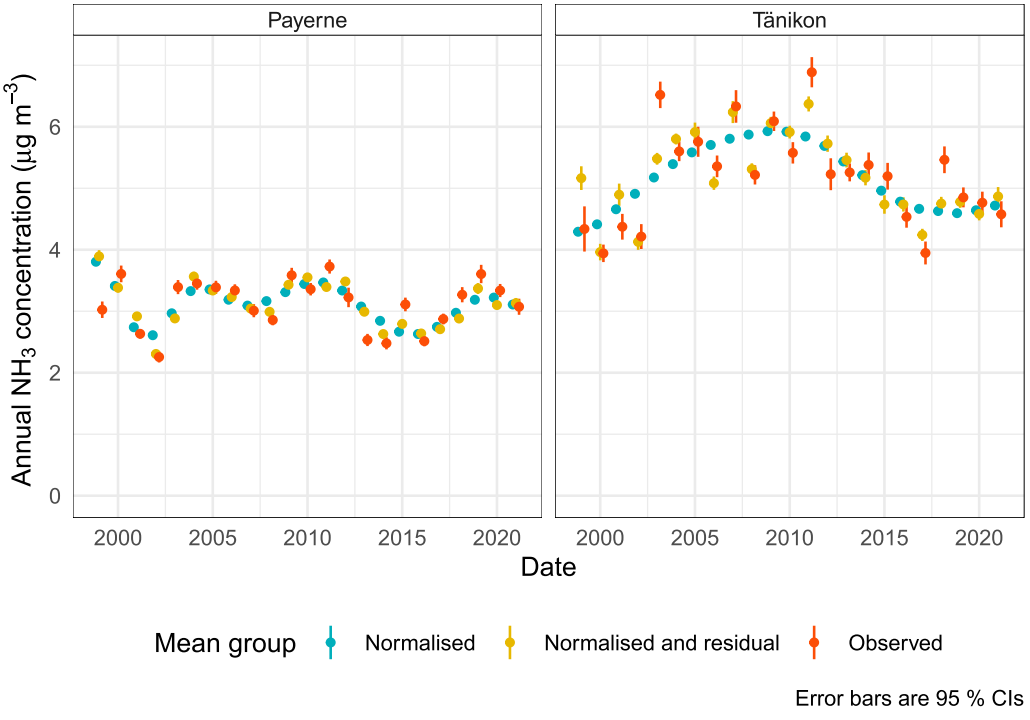


**Fig. 3.** An example of the reduction of variability the GAM procedure achieves for $NH_3$ annual means at Payerne and Tänikon – two rural locations in Switzerland between 1999 and 2021.

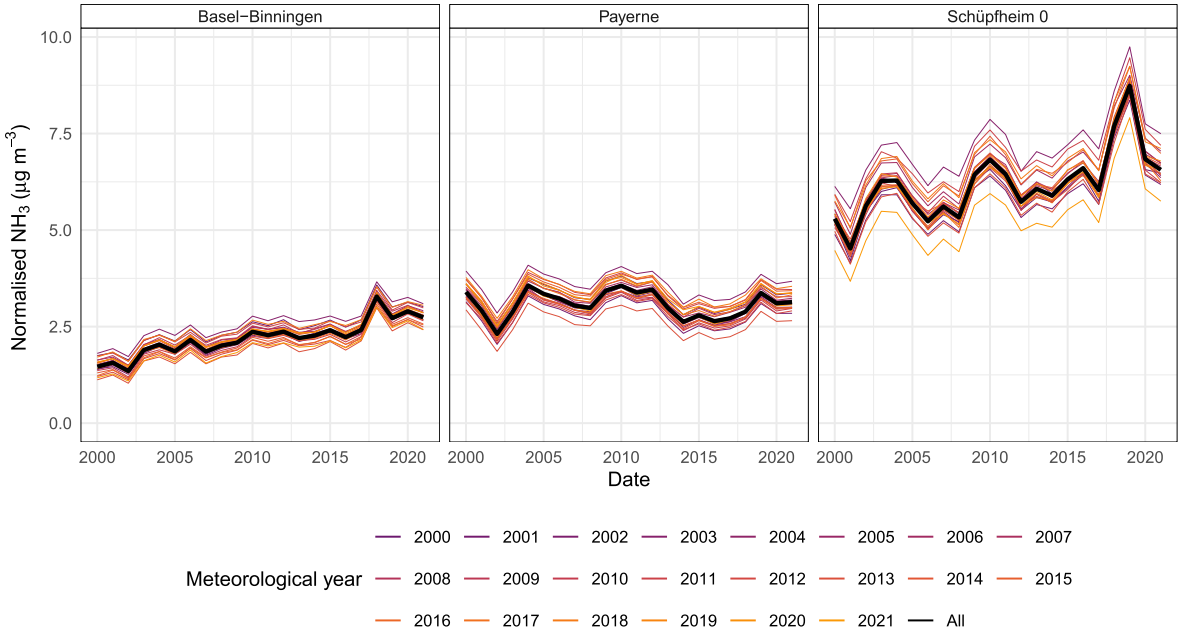


**Fig. 4.** Examples from Basel-Binningen, Payerne, and Schüpfheim 0 of the many normalised time series using sampled meteorological input variables for each year after 2000 in the sampling record. The bold line represents the mean of all years and was considered the average prediction.

of hourly time series for each $NH_3$ sampling location, the transformation of many of the supplied variables into variables that were suitable for analysis (for example, *u* and *v* wind components to wind speed and direction), the isolation of the hourly time series for a particular $NH_3$ sampling period (generally 14 or 28 days), and finally the aggregation of this sampling period to represent the average meteorological conditions for each $NH_3$ sampling period. The result was a synchronous dataset of $NH_3$ observations, average air temperature, atmospheric pressure, boundary layer height, precipitation, relative humidity, downwards solar radiation, wind speed, wind direction, the number of precipitation hours, the sum of precipitation, and the maximum duration of consecutive dry days (CDD), which were defined as days with less-than 1 mm of precipitation.

### 2.2. Modelling

#### 2.2.1. Controlling for the influence of weather

To control for the influence of weather on the $NH_3$ time series to improve trend estimates, several steps were required to prepare the time series. These steps included the training of regression models, sampling, prediction, and aggregation. The procedure is outlined below.

Separate generalised additive models (GAMs) were calculated for each of the 32 $NH_3$ sampling locations for the period where observations were available. $NH_3$ concentrations were modelled using air temperature, relative humidity, atmospheric pressure, boundary layer height, precipitation, CDDs, wind direction, wind speed, Unix date (number of seconds since 1970-01-01), and Julian day (day of the year 1–366). The sample durations' means were used for the meteorological independent variables, with the exception of precipitation and CDDs where the sample durations' sum and maximum were used respectively. All independent variables were modelled with smooth terms in the GAMs with cubic splines. The number of knots was set to the default value of nine for all variables apart from CDDs because of the very few numbers of unique values for some sampling periods, and Julian day where the number of knots was set to 20 to allow for additional "wiggliness" that was required to better represent the seasonal cycle of $NH_3$ concentrations. However, the restricted maximum likelihood (REML) smoothing method was employed that can iteratively adjust smoothing parameters if the model fails to converge. The GAM modelling was conducted using the **mgcv** R package (Wood, 2011; R Core Team, 2019).

The chosen set of independent variables was determined by running 1500 models with different independent variable combinations and evaluating the models' $R^2$ values and the best model formulation was selected. The correlation of independent variables was also tested to avoid multicollinearity within the GAMs. At this step, incoming solar radiation was removed from the model formulation because it was well correlated with air temperature and on average, air temperature was a superior predictor. The models' residuals were approximately normal, but the GAMs were unable to accurately predict peak $NH_3$ values at most sampling locations. The modelling was not conducted with log-transformed $NH_3$ concentrations, unlike some other previous works (Thöni et al., 2004; Philipp and Locher, 2010; Häni and Kupper, 2021). The use of log-transformed concentrations was tested, however, and it was found that using transformed dependent variables did not systematically improve model performance and only made minor improvements to the normality of the models' residuals' distributions. The models' residual diagnostic plots can be found in a persistent data repository (Grange, 2022b). As a final validation step, the models' partial dependencies were investigated to ensure the GAMs were using the independent variables in an intuitive and understandable manner. The average $R^2$ of the models was 62.4 % with a maximum of 86.9 %. Three model error metrics for all 32 models are shown in Fig. A3.

After the GAMs were trained and validated, they were used to control for the influence of changes in weather on $NH_3$ concentrations during the sampling period (1999–2021). First, all independent variables except Unix date (the trend term) were sampled with replacement to create a randomly shuffled set. Second, the GAM was used to predict $NH_3$ concentrations with the shuffled set. This is the same logic implemented in the meteorological normalisation approach (Grange et al., 2018; Grange and Carslaw, 2019), but this method usually uses a random forest model. However, here, an additional piece of logic was introduced where each calendar year was sampled and predicted individually to allow for investigations into the difference among the years (Lang, 2020). For the cases where the passive sampling tube period traversed two calendar years (1.7 % of the observations), these samples were included in both years. For each year where observations were available, the sample-predict process was repeated 100 times and summarised at the arithmetic mean to create a normalised time series

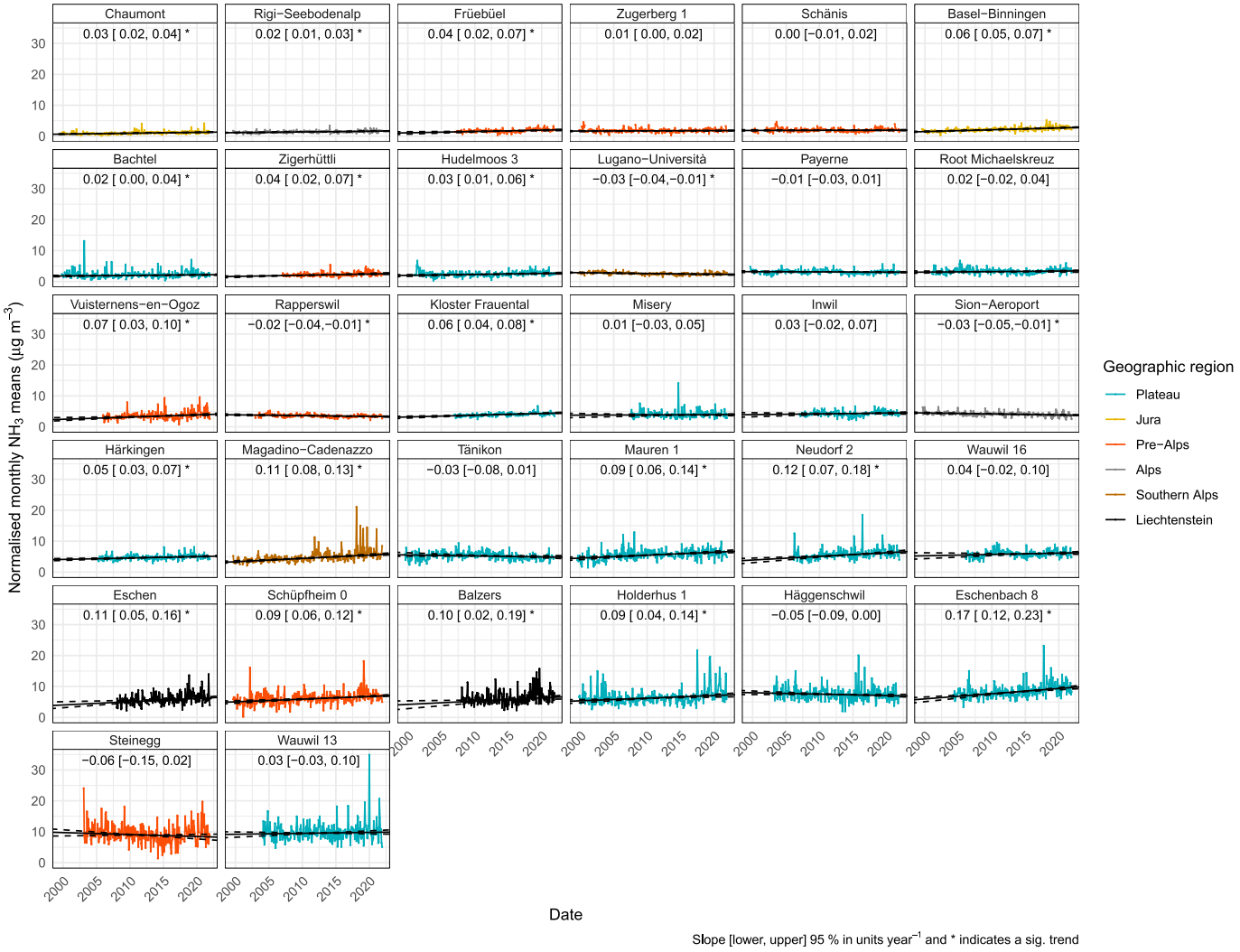


**Fig. 5.** Normalised $NH_3$ trends between 2000 and 2021 for 32 sampling locations in Switzerland and Lichtenstein. The sites are ordered by their mean $NH_3$ concentration.

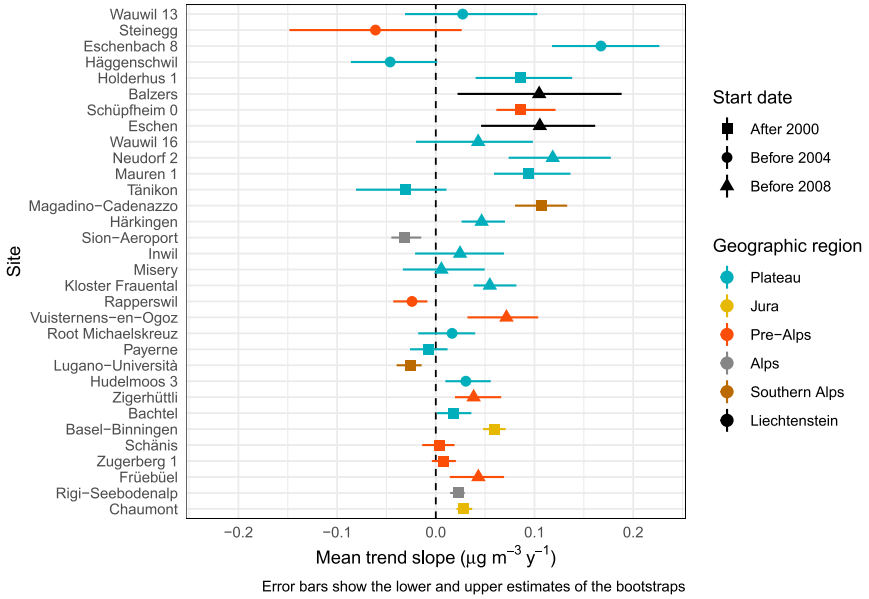


**Fig. 6.** $NH_3$ trend slopes between 2000 and 2021 for 32 sampling locations in Switzerland and Liechtenstein. The sites are ordered by their mean $NH_3$ concentration.

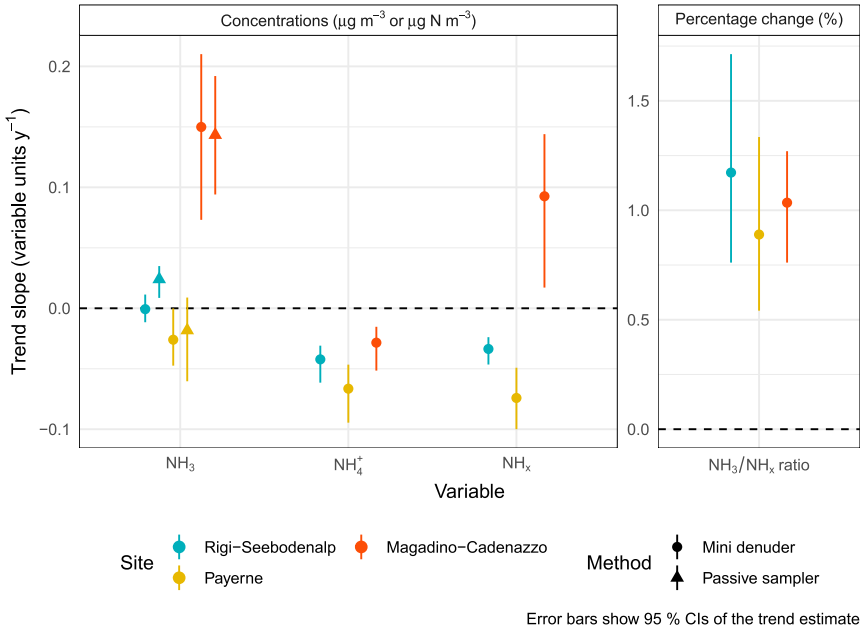


**Fig. 7.** Trend slopes of $NH_x$, $NH_3$, $NH_4^+$, and $NH_3/NH_x$ ratio between 2007 and 2021 for three sampling locations where mini denuders were operated. The $NH_x$ units are g N m-3.

representing $NH_3$ concentrations in "average weather" for the entire sampling period. Because the GAMs cannot represent all processes that influence $NH_3$ concentrations and indeed represent the processes that are present imperfectly, the model residuals were added to the normalised time series and this final product can be expressed as the trend plus remainder. No sites were excluded from the analysis due to poor GAM model performance because even with poorer than desired model performance, some of the variability driven by meteorology was removed and this reduction still helped in the trend analysis procedure. GAMs were chosen over the random forest algorithm because, during testing, GAMs had a superior performance for the passive sampler data set where several hundred observations were available, rather than several thousand observations typically found for datasets formed by online measurements.

The trends of $NH_3$ were tested using the robust and non-parametric Theil-Sen slope estimator (Wilcox, 2004; Carslaw and Ropkins, 2012). The trend tests were conducted at the 0.05 significance level and block bootstrapping was applied to allow the calculation of uncertainty around the slope and intercept coefficients. Although some $NH_3$ sampling locations commenced sampling in 1999, the trend analysis period began at the start of 2000 to avoid introducing a partial year of observations for some of the time series.

### 2.2.2. *Partitioning of gas and aerosol phases*

The ISORROPIA II thermodynamic equilibrium model (Fountoukis and Nenes, 2007) was used to model the $NH_3$ - $NH_4^+$ gaseous and particle phase system in 30 locations across Switzerland and two locations in Liechtenstein (Table 1). ISORROPIA II was run in forward mode and the **isorropiar** interface was used to interact with ISORROPIA II's input and outputs (Grange, 2022a).

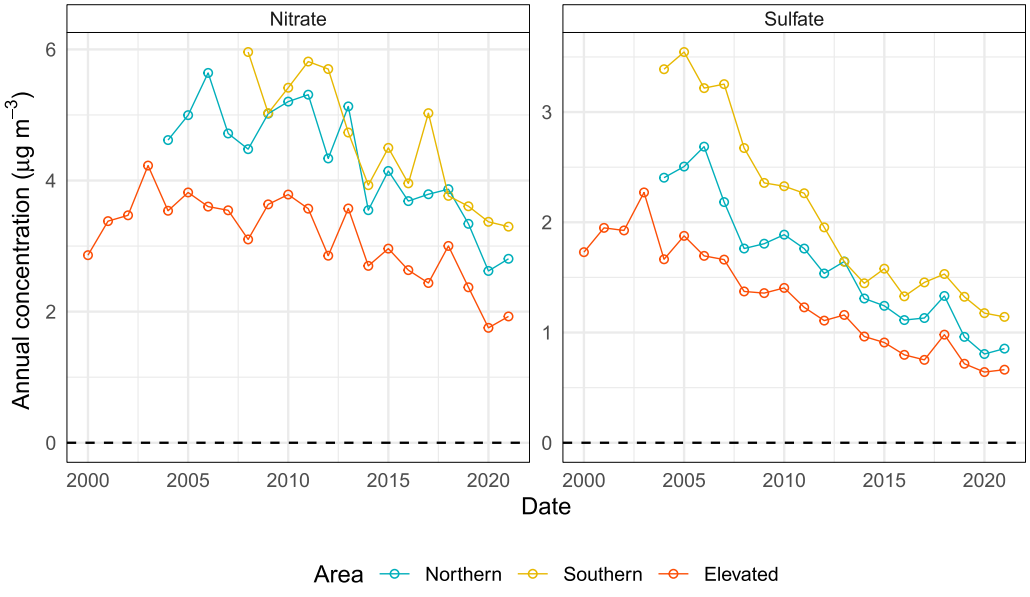


**Fig. 8.** Annual means of nitrate ($NO_3^-$) and sulfate ($SO_4^{2-}$) for three representative locations across Switzerland between 2000 and 2021.

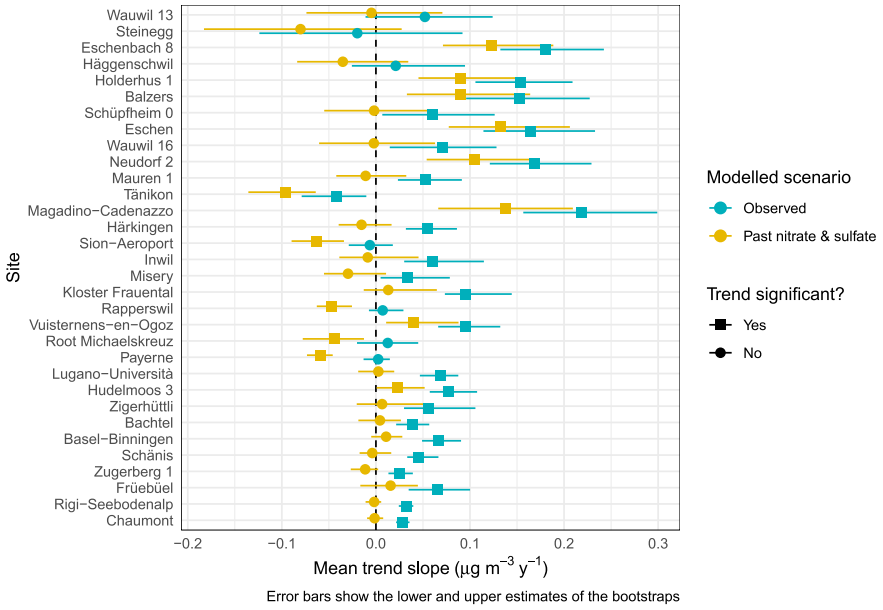


**Fig. 9.** ISORROPIA II-derived $NH_3$ trend slopes between 2004 and 2021 for 32 sampling locations in Switzerland and Liechtenstein. The sites are ordered by their mean $NH_3$ concentration.

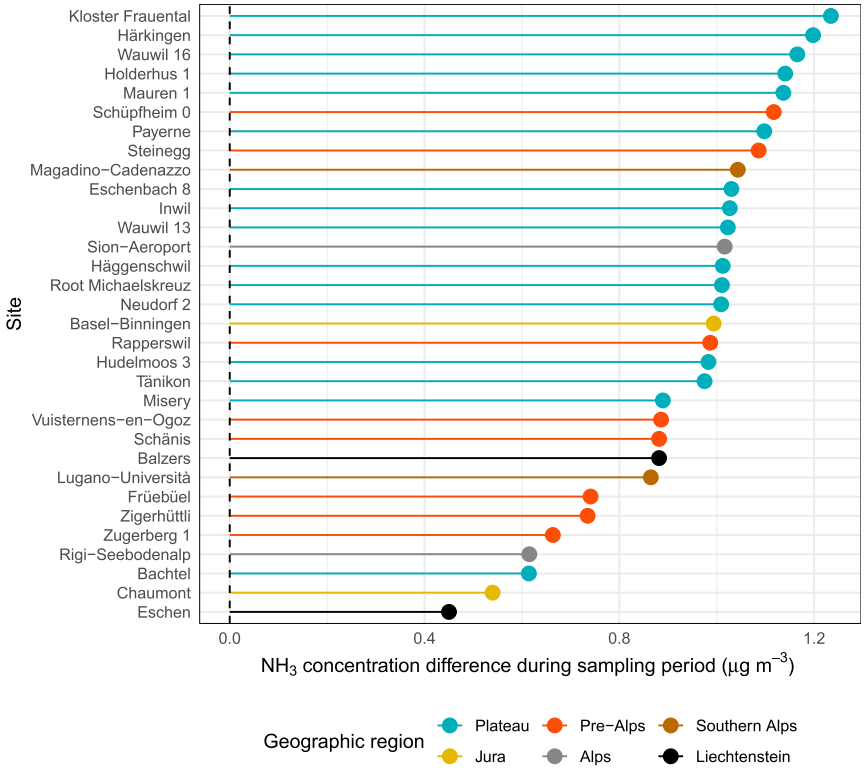


**Fig. 10.** Differences in $NH_3$ concentrations for 32 sampling locations between 2004 and 2021 based on the locations' mean trend estimates of what was observed and what was simulated using past nitrate ($NO_3^-$) and sulfate ($SO_4^{2-}$) concentrations.

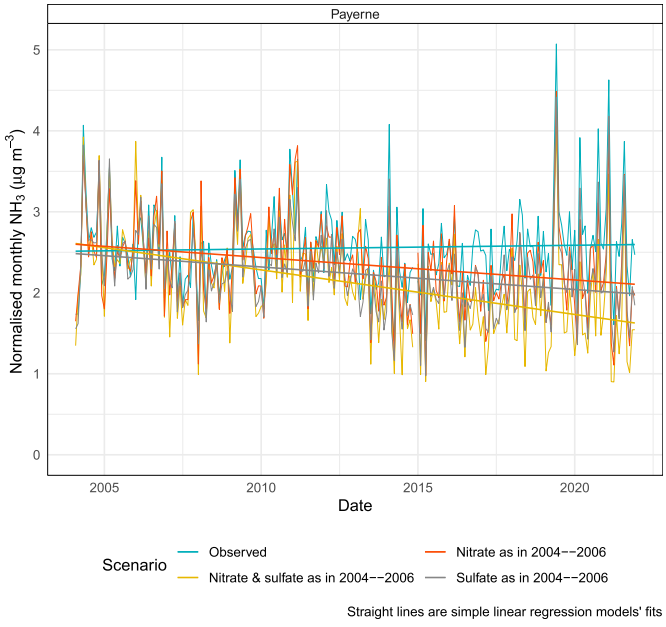


**Fig. 11.** Normalised $NH_3$ concentrations for the observed time series and three ISORROPIA II scenarios based on past nitrate ($NO_3^-$) and sulfate ($SO_4^{2-}$) concentrations for Payerne between 2004 and 2021.

ISORROPIA II requires a number of species to be supplied to correctly resolve the $NH_3$ - $NH_4^+$ partitioning and in most locations where passive $NH_3$ sampling tubes were installed, data for these additional species do not exist. Therefore, representative "northern", "southern", and "elevated" time series were constructed for the simulations. A representative time series here refers to one containing homogeneous concentrations of secondary inorganic PM species experienced within the three defined areas. This assumption was justified because the concentrations of such species have been found to be very similar across Switzerland's geographic areas (Grange et al., 2021). The northern time series used observations from Payerne and covered a period between 2004 and 2021, the southern time series used a combination of Magadino-Cadenazzo and Lugano-Università data that began in 2009 and ran to 2021, and finally, the elevated time series used observations from Rigi-Seebodenalp and like the northern time series ran between 2004 and 2021. For full clarity, Table A1 contains the details of what representative data were used for each location and what time periods the observations covered. For all ISORROPIA II model runs, the input time series was at monthly resolution.

Two groups of ISORROPIA II models were run: the first used observed concentrations of the input species required for the modelling, and the second was a synthetic set where the $SO_4^{2-}$ and $NO_3^-$ concentrations were fixed at their past concentrations, generally 2004 and 2006, but there was some shifting of this past period due to site-specific data availability (see Table A1 for full details). The synthetic sets represented past concentrations of two ions that represent $HNO_3$ and $H_2SO_4$ which are key species that dictate the partitioning of $NH_3$ - $NH_4^+$.

After modelling with ISORROPIA II, a model validation step was conducted to test whether the reconstituted $NH_3$ concentrations were correct and thus suggested that the representative time series were appropriate for each $NH_3$ sampling location. Scatterplots comparing observed and ISORROPIA II modelled $NH_3$ monthly means for example sites are shown in Fig. A4. Admittedly, using monthly observations for scenario modelling of this type is sub-optimal and observations at say, hourly resolution would be preferable. However, based on Fig. A4, the ISORROPIA II model was able to reconstitute $NH_3$ from the model's input data in all three representative environments very well. This gives evidence that although we do not have access to high-resolution observations (because these data do not exist), monthly simulations can be used with confidence in further analysis of $NH_3$ concentrations.

Once the ISORROPIA II modelled $NH_3$ monthly means were validated, the time series were subjected to the same controlled-for-meteorological trend analysis (Section 2.2.1) to allow for all trend estimates in this work to be calculated in the same way. However, the meteorological variables were joined using calendar-month periods and the trends were calculated for the period where ISORROPIA II outputs were produced.

## 3. Results and discussion

### 3.1. $NH_3$ concentration summaries

Atmospheric $NH_3$ concentrations in Switzerland between 2000 and 2021 were variable among the sampling sites included in the analysis. Sampling locations in areas with intensive livestock farming had the highest mean and greatest peak $NH_3$ concentrations (Fig. 2). Most of these polluted sampling sites are located on the Swiss plateau and in the pre-Alps, the two geographic regions with the most intensive agricultural activities in Switzerland (Bundesamt für Statistik, 2021; Federal Office for the Environment, 2021). In areas where mainly arable farming is practised, as well as in urban and suburban environments, mean and peak $NH_3$ concentrations were lower. The two sampling locations in Liechtenstein were also within the ten most polluted sampling locations. The two least polluted $NH_3$ locations were Chaumont and Rigi-

**Table A1**
Details on what datasets were used for what sites for the ISORROPIA II modelling. Note that what is defined as "past" changes depending on what site is being discussed due to limitations of data coverage.

| Simulation | Location | Past years | Sites |
|---|---|---|---|
| Observed | Northern | | Payerne, Basel-Binningen, Eschenbach 8, Häggenschwil, Holderhus 1, Hudelmoos 3, Mauren 1, Rapperswil, Root Michaelskreuz, Schänis, Schüpfheim 0, Sion-Aeroport, Steinegg, Tänikon, Wauwil 13, Härkingen, Vuisternens-en-Ogoz, Neudorf 2, Wauwil 16, Inwil, Kloster Frauental, Misery, Balzers, Eschen |
| Observed | Southern | | Lugano-Università, Magadino-Cadenazzo |
| Observed | Elevated | | Bachtel, Chaumont, Früebüel, Rigi-Seebodenalp, Zigerhüttli, Zugerberg 1 |
| Past nitrate & sulfate | Northern | 2004, 2005, 2006 | Payerne, Basel-Binningen, Eschenbach 8, Häggenschwil, Holderhus 1, Hudelmoos 3, Mauren 1, Rapperswil, Root Michaelskreuz, Schänis, Schüpfheim 0, Sion-Aeroport, Steinegg, Tänikon, Wauwil 13, Härkingen, Vuisternens-en-Ogoz, Neudorf 2, Wauwil 16, Inwil, Kloster Frauental, Misery, Balzers, Eschen |
| Past nitrate & sulfate | Southern | 2009, 2010, 2011 | Lugano-Università, Magadino-Cadenazzo |
| Past nitrate & sulfate | Elevated | 2004, 2005, 2006 | Bachtel, Chaumont, Rigi-Seebodenalp, Zigerhüttli |
| Past nitrate & sulfate | Elevated | 2007, 2008, 2009 | Früebüel, Zugerberg 1 |

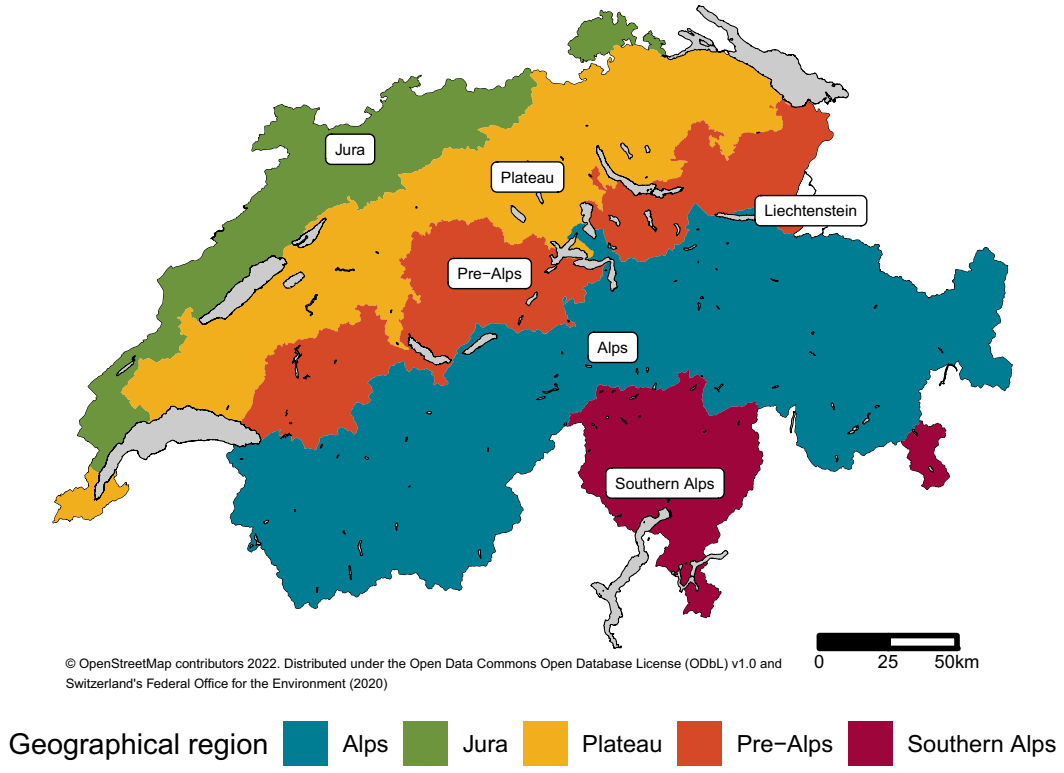


**Fig. A1.** The extent of Switzerland's five geographical regions (and Liechtenstein). Polygons are from Federal Office for the Environment (2020) and the filled grey areas represent significant lakes and reservoirs.

Seebodenalp, both elevated and somewhat isolated mountain sites at over 1000 m of elevation (Table 1; Fig. 1).

The $NH_3$ time series (Fig. A5) shows that all sites experienced highly variable concentrations during their sampling duration with isolated peaks of high concentrations. Such events most likely represented periods where high emissions from nearby agricultural activities coincided with either wind directions that favoured $NH_3$ transport to the nearby sampling tubes, or periods where atmospheric dispersion and transportation were low. The most polluted sites, including Wauwil 13, Steinegg, and Eschenbach 8 (all on the Swiss plateau or in the pre-Alps), all experienced low $NH_3$ concentrations at times, but the minimum concentrations experienced were higher than the less polluted locations. This enhanced minimum is indicative of the increased regional loading of $NH_3$ in such locations and can be demonstrated even for a short-lived pollutant such as $NH_3$.

Fig. A5 also shows the durations of when the three different types of passive sampling tubes were in operation. Among the three sampler types that were used between 2000 and 2021, no dramatic shifts were observed in $NH_3$ concentrations. However, for some of the more polluted locations, such as Magadino-Cadenazzo, Mauren 1, Holderhus 1, and Eschenbach 8, the change to the Ferm sampler (the change in sampler usually occurred in 2019) somewhat corresponded with increases in minimum (and average) $NH_3$ concentrations. In other locations, including other less and more polluted sites, this effect was not observed. The different sampler types have been exposed to intensive comparisons and these results show very good agreement between sampler types (Seitler and Meier, 2022), thus giving confidence that the increase in baseline concentrations was not an artefact of changing sampler type. Additionally, in the case of Magadino-Cadenazzo, alternative $NH_3$ sampling techniques (an $NH_3$ gas analyser and a mini denuder) show the same increases in concentrations as the diffusion tubes, thus giving evidence that the increase in $NH_3$ concentrations by the Ferm sampling tubes during and after 2018 reflect increasing $NH_3$ concentrations at this location and this is discussed further below.

### 3.2. Trend analysis

The goal of controlling the $NH_3$ time series for weather was to reduce the influence of both the atmospheric dispersion characteristics on concentrations and weather-driven changes in emission processes. The reduction of such variability uncovers the changes in emissions more clearly and increases the power of statistical tests of trends due to the errors being smaller.

Examples of the reduction in variability are displayed in Fig. 3 where $NH_3$ annual means for the Payerne and Tänikon rural sampling locations are shown. The observed annual means demonstrate significant year-to-year variability, partially due to the changeable state of atmospheric dispersion characteristics and the impacts of meteorological conditions on $NH_3$ generation during the 1999–2021 sampling period. Once the time series has been normalised (or controlled) for meteorology over time, the intra-annual variability was substantially reduced. However, because the GAM modelling procedure cannot perfectly remove the influence of meteorology, the models' errors were added to the predictors that resulted in the normalised and remainder time series. The annual means of for example 2018, showed the reduction of variability clearly and the high concentrations of $NH_3$ were driven by high ambient air temperatures and drought conditions that were experienced across Switzerland during this year.

Normalising the $NH_3$ trends by every calendar year contained in the observational record allowed for the evaluation of the amount of variation in $NH_3$ concentration that can be attributed to the meteorological conditions of a given year. Fig. 4 shows three sampling sites and demonstrates the range of predictions by each year between 2000 and 2021. The "bundle" of predictions show what $NH_3$ concentrations could be expected based on the weather conditions experienced within a year for a sampling location. The average amount of variation of the annual mean among the sampling years was 33 %. This mean variation of 33 % is substantial and suggests that given identical $NH_3$ emissions for any given year, the influence of weather-driven processes could change

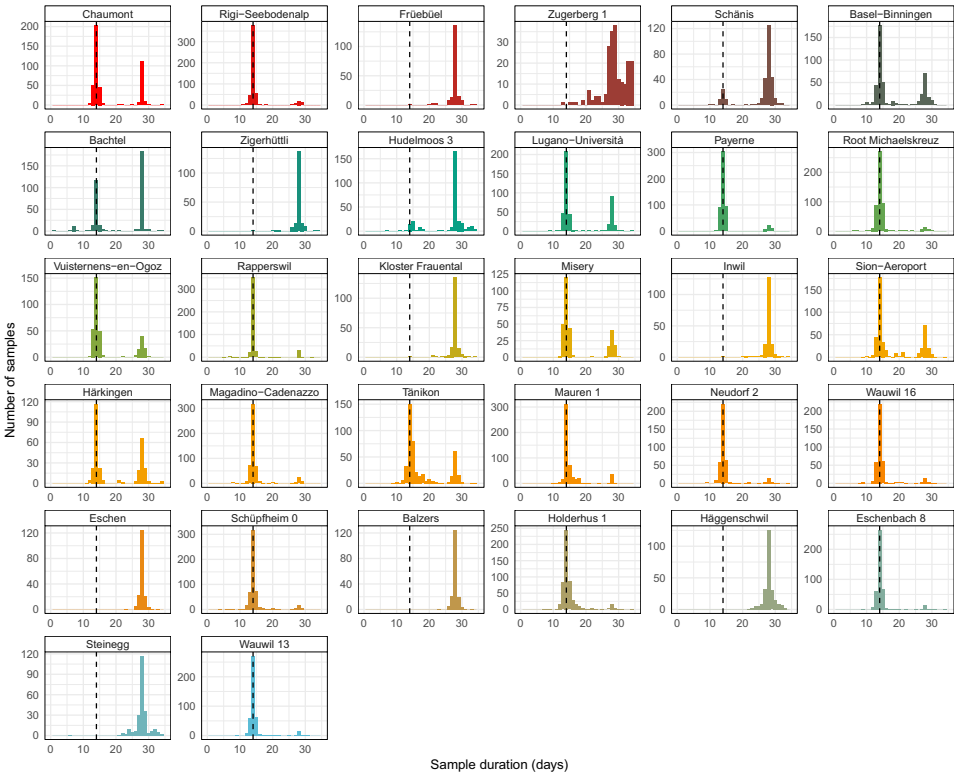


**Fig. A2.** Histograms of the passive sampler $NH_3$ sample durations for the 32 locations included in the analysis. The majority of samples were of two-week duration, but four-week samples were also common for some sampling years.

observed concentrations by up to a third.

Once the $NH_3$ time series were prepared to control for the changes in meteorology over the 2000–2021 sampling and analysis period, much of the short-term variation in $NH_3$ concentrations was removed. The results in Fig. 5 show the sum of the trend component and the models' residuals to more clearly represent the trends of $NH_3$ concentrations over time. The results of the formal trend tests are also printed in the upper section of Fig. 5's panels with the units of $\mu g\ m^{-3}\ y^{-1}$.

The first noticeable feature of the trend analysis shown in Fig. 5 is the lack of obvious decreasing trends of $NH_3$ concentrations across Switzerland and Liechtenstein during the analysis period. Twenty-nine of the 32 sites (91 %) had either statistically insignificant or significantly increasing trends of $NH_3$ between 2000 and 2021. The three sites with significantly decreasing trends were Sion-Aeroport (next to a motorway) and the only two urban sites Lugano-Università and Rapperswil, and their trends ranged from $-0.02$ to $-0.03\ \mu g\ m^{-3}\ y^{-1}$. Seventeen sites had significantly increasing trends that ranged from 0.02 (at Bachtel and Rigi-Seebodenalp) to $0.17\ \mu g\ m^{-3}\ y^{-1}$ (at Eschenbach 8). Both of the sampling locations in Liechtenstein showed significant increasing trends and their $NH_3$ time series commenced in 2008.

The $NH_3$ trend estimates are shown in Fig. 6 and it is immediately noticeable that the weight of the $NH_3$ trends are in the positive direction. It is also observable that there is a tendency for the more polluted sites to be more likely to have positive trends at a greater magnitude. To put the $NH_3$ trends into context with other $NH_x$ species, observations from mini denuders were exposed to the same method to control for changes in weather using GAMs and prediction that the passive samplers were. There are three locations in Switzerland where the mini denuders were active and the sampling period was shorter because their operation started in 2007. Fig. 7 shows the trend slopes between 2007 and 2021 for the three mini denuder sites including the passive sampler trends for $NH_3$ as well.

The $NH_3$ trends calculated for the two sampling methods were similar with the mini denuder estimates having less error due to the increased sampling rate and therefore, an increased number of samples were available for the modelling process and trend tests. The $NH_3$ trend at Rigi-Seebodenalp determined by the mini denuder was insignificant, but the passive sampler trend showed significantly increasing trends (Fig. 7). The error bars of the two trend estimates do overlap, but at this location, there was a difference in the $NH_3$ trend estimate between the two sampling methods.

In contrast to $NH_3$, the mini denuder samples show that $NH_4^+$ concentrations significantly decreased between 2007 and 2021 across the Swiss plateau (Fig. 7). This significant decrease was even present at Magadino-Cadenazzo where $NH_3$ concentrations increased rather rapidly during the same time period. $NH_4^+$ concentrations have been found to be rather homogeneous across Switzerland (Hüglin and Grange, 2021; Grange et al., 2021) and the processes that drive this PM component include larger scale regional processes that are rather different to those that influence gaseous $NH_3$. $NH_x$ (the sum of $NH_3$ and $NH_4^+$) decreased between 2007 and 2021 at the two sites located north of the Alps. However, because $NH_3$ concentrations are increasing more rapidly at Magadino-Cadenazzo, the $NH_x$ trend estimate is also significantly increasing.

The critical conclusion of the $NH_x$ trends in Fig. 7 is that the $NH_3/NH_x$ ratio has changed in Switzerland with a tendency of a greater proportion of $NH_x$ being composed of $NH_3$, even when $NH_4^+$ concentrations are decreasing over time. This suggests that the chemical processes that govern the partitioning between $NH_3$ and $NH_4^+$ have changed over time leading to an increasing $NH_3/NH_x$ ratio across Switzerland. $NH_3$ emissions in Switzerland have been subject to significant control efforts, but despite the management policies, $NH_3$ concentrations have not decreased due to the atmospheric chemistry changes that have occurred as $NH_3$ sinks have progressively decreased. Therefore, this creates a situation where increasing $NH_3$ concentrations can be observed, even when $NH_3$ emissions remain constant or even decrease.

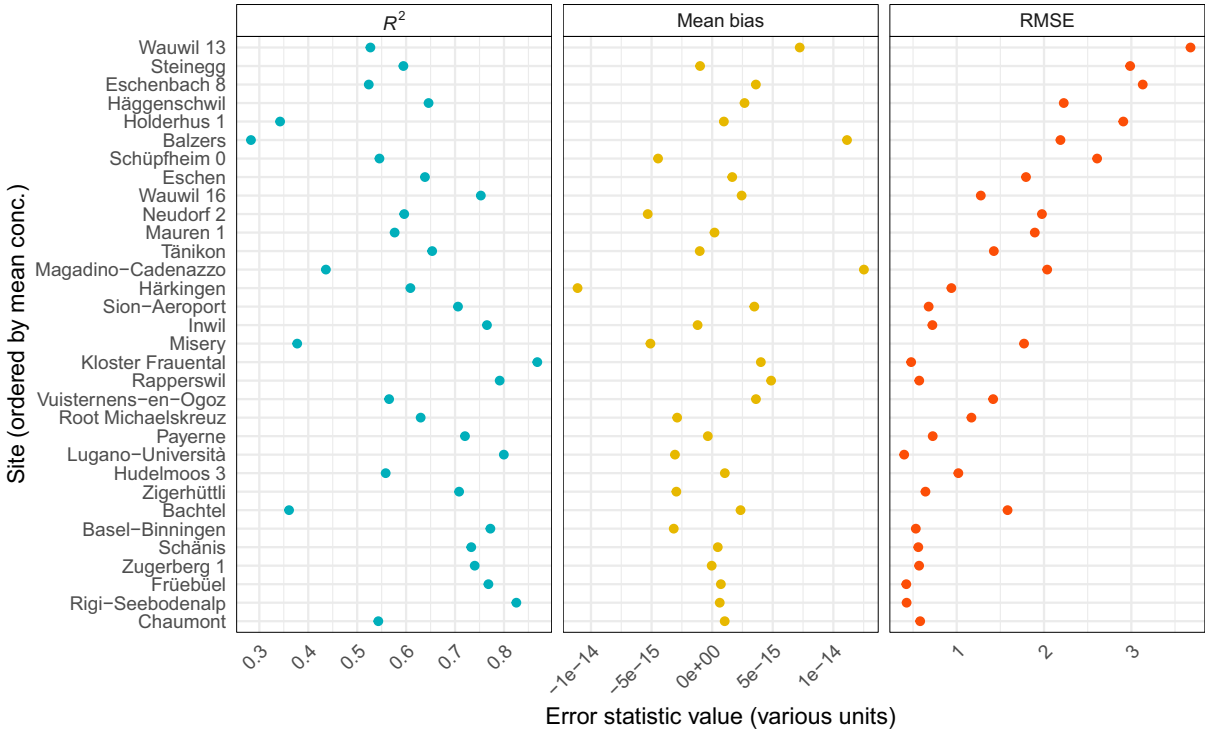


**Fig. A3.** Model error statistics for the 32 $NH_3$ GAMs used for the analysis. The sites have been ordered by their mean $NH_3$ concentration.

### 3.3. $NH_3$ - $NH_4^+$ partitioning investigation

To investigate the causes of why $NH_x$ has decreased across much of the Swiss plateau while $NH_3$ concentrations have increased during this study's analysis period, the ISORROPIA II thermodynamic equilibrium model (Fountoukis and Nenes, 2007) was used to investigate the influence of the reduction of the $NH_3$ sinks, *i.e.*, $HNO_3$ and $H_2SO_4$ on the $NH_3$ - $NH_4^+$ partitioning. Synthetic datasets were constructed that were compared to the observational records to determine the effect of changes in the acids on ambient $NH_3$ concentrations for where passive $NH_3$ samples were taken.

$NO_3^-$ and $SO_4^{2-}$ concentrations have decreased across Switzerland between 2000 and 2021 (Fig. 8) and these inorganic particulates are predominantly products of the reaction of $NH_3$ with $HNO_3$ and $H_2SO_4$ and can be thought of as representative of the availability of these two acids. Therefore, these two acids that are $NH_3$'s greatest atmospheric sinks have decreased across Switzerland during this study's analysis period (2000−2021).

The $NH_3$ passive sampler trend analysis (Section 3.2) showed that only three of the 32 sampling sites experienced significantly decreasing trends across their sampling periods. For example, Payerne had a trend that was insignificant between 2000 and 2021 (Fig. 5; Fig. 6). However, when the mean monthly $NO_3^-$ and $SO_4^{2-}$ concentrations that were experienced in 2004–2006 were used for the 2004–2020 observational record, a significantly decreasing trend of 0.06 $\mu g\ m^{-3}\ y^{-1}$ in $NH_3$ was determined (Fig. 9). This gives evidence that the reduction of acids across the Swiss atmosphere has altered the $NH_3$ - $NH_4^+$ partitioning system towards less $NH_4^+$ formation and therefore, more $NH_3$ in the gas phase. The shift towards a higher $NH_3/NH_x$ ratio was observed at three locations with mini denuder samplers too (Fig. 7). In other locations that were more polluted with $NH_3$ the loss of the acid sinks over time did not change the trend estimate from insignificant to significantly negative but did nevertheless push the trend estimate downwards (towards a flat or negative trend). For some sites, the observed trends in Fig. 6 and Fig. 9 are slightly different. This occurred because the time period used for the ISORROPIA II modelling was shorter for some of the long-running sites (see Section 2.2.2 for details).

To quantify the effect of the reductions of the $HNO_3$ and $H_2SO_4$ sinks on $NH_3$ trends during the time when passive sampling was taking place, the differences between the observed $NH_3$ trend slopes were compared to the slopes calculated from the synthetic datasets using higher past $NO_3^-$ and $SO_4^{2-}$ concentrations. Fig. 10 shows the differences between the two trend estimates between the 2004 and 2021 period, not by year. The mean effect of reduced $HNO_3$ and $H_2SO_4$ concentrations on $NH_3$ concentrations was 0.9 $\mu g\ m^{-3}$ and ranged from a minimum of 0.45 $\mu g\ m^{-3}$ at Eschen (Liechtenstein) to a maximum of 1.2 $\mu g\ m^{-3}$ at Kloster Frauental for the period between 2004 and 2021. Additionally, there was no clear dependence between calculated sink reductions and mean $NH_3$ concentrations between 2004 and 2021, except that the calculated sink reductions were smallest at elevated sites, where the ambient concentrations of $NO_3^-$ and $SO_4^{2-}$ are at their lowest (Fig. A6; Fig. A7).

The magnitude of the effect of sink reductions on the $NH_3$ trends across Switzerland between 2004 and 2021, was on average, 0.9 $\mu g\ m^{-3}$. This means that today's ambient $NH_3$ concentrations would be lower (on average) by this amount when the concentration of acids would have remained at the levels of 2004. To put the effect in context, mean concentrations of $NH_3$ across Switzerland ranged from 1.0 and 9.9 $\mu g\ m^{-3}$ among the sampling sites included in this analysis. In areas of intensive livestock farming, the highest annual averages have been reported as 12 $\mu g\ m^{-3}$ by others (Seitler and Meier, 2022). The effect of the sink reductions in the past on ambient $NH_3$ concentrations is therefore rather substantial, even more so for sites with lower concentrations.

A striking difference between the observed monthly $NH_3$ and the synthetic time series calculated with past ion concentrations was that the synthetic time series showed during some winter months at many sampling sites, $NH_3$ concentrations were predicted to be zero (for example, Fig. A8). This feature can be explained by the greater concentrations of sinks that were available in the synthetic time series and that were great enough to completely deplete $NH_3$ during some winter

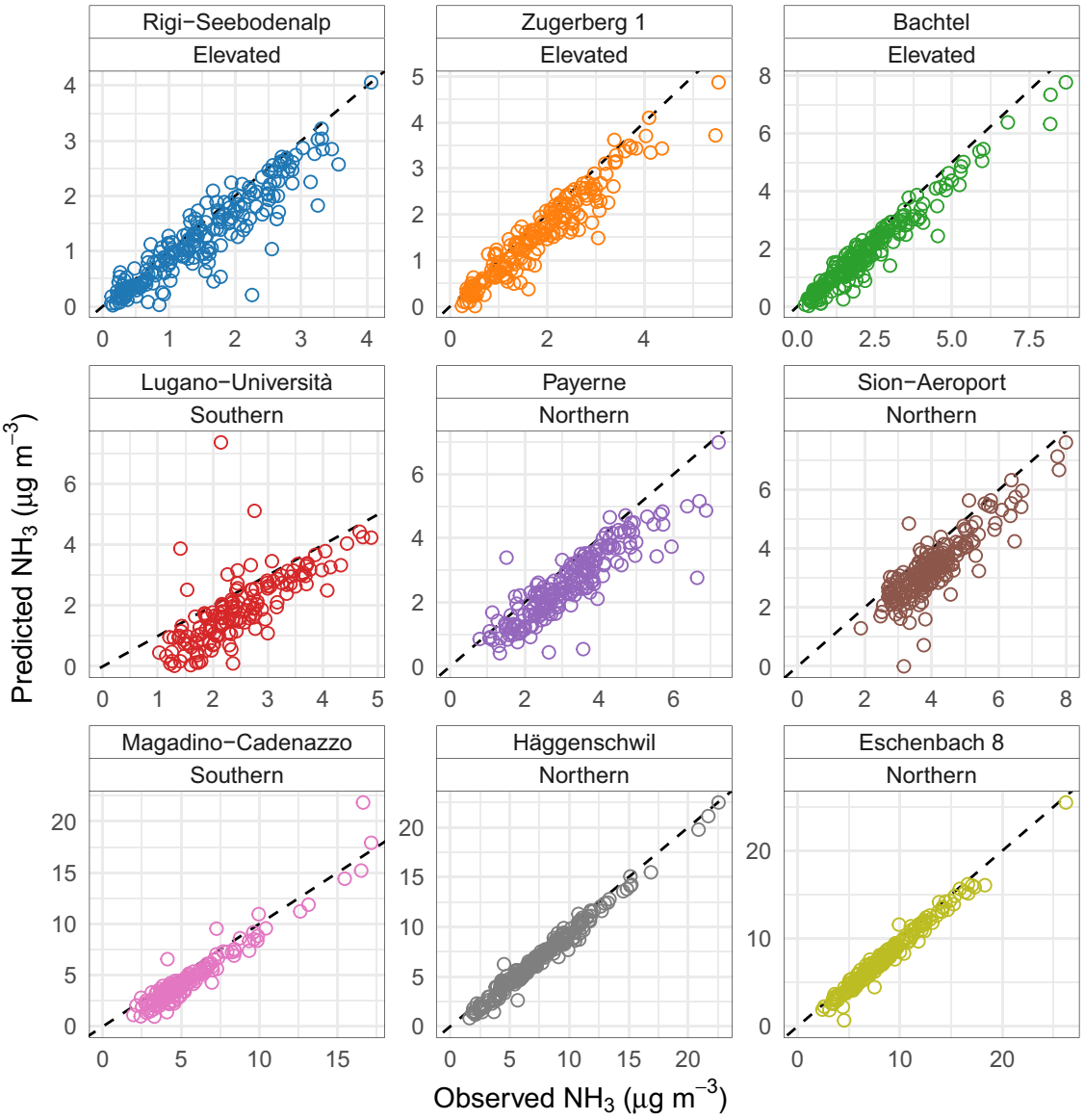


**Fig. A4.** Predicted and observed $NH_3$ concentrations between 2004 and 2021 from the ISORROPIA II model for six sampling locations with different mean $NH_3$ concentrations and covering the three sets of representative time series (northern, southern, and elevated).


**Fig. A5.** $NH_3$ time series for 32 passive sampler locations in Switzerland and Liechtenstein between 2000 and 2021. The sites are ordered by their mean $NH_3$ concentration.

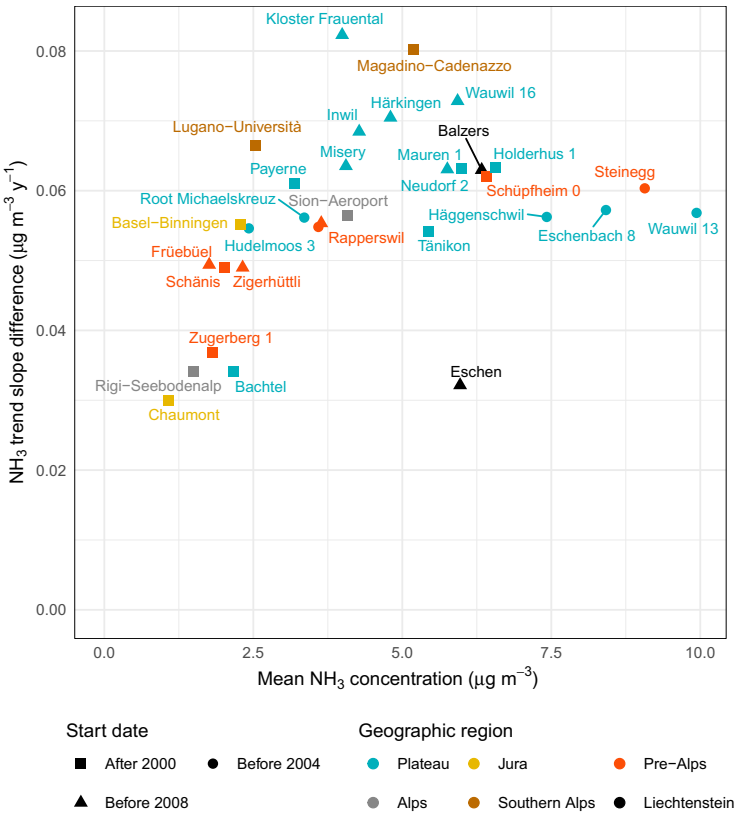


**Fig. A6.** Scatterplot of mean $NH_3$ concentrations (between 2004 and 2021) and the difference of $NH_3$ trend estimates for 32 sampling locations between what was observed and what was simulated using past nitrate ($NO_3^-$) and sulfate ($SO_4^{2-}$) concentrations.

months. ISORROPIA II modelling was also conducted with perturbing $NO_3^-$ and $SO_4^{2-}$ individually and it was not clear what ion had a stronger effect on the $NH_3$ - $NH_4^+$ partitioning process on average. However, some locations did show that $SO_4^{2-}$ was the more potent ion (for example, Fig. 11; Fig. A9), perhaps due to the transformation to ammonium sulfate (or bisulfate) is an irreversible process, unlike the transformations to ammonium nitrate (Renner and Wolke, 2010).

## 4. Conclusions

The processes discussed above were able to be illuminated due to the long-term and high-quality atmospheric sampling and monitoring activities across Switzerland since 2000. However, the implications of the findings extend well beyond Switzerland to many European locations and are very likely relevant and important to consider in other European countries. Indeed, all countries surrounding Switzerland and Liechtenstein show similar behaviour in their reported $NH_3$ emissions (Fig. A10). The investigation of the increase in the $NH_3/NH_x$ ratio due to a reduction of sinks is worthy of investigation in other locations where $NH_3$ emissions and concentrations appear to be somewhat disconnected, especially where $NH_3$ emission control is active, but ambient concentrations have failed to decline in line with the calculated emission reductions. This analysis also shows that there is substantial value in monitoring or sampling at least two of the $NH_x$ - $NH_3$ - $NH_4^+$ triad in parallel to get a more complete understanding of $NH_x$ at a particular location. The extra information gained by using mini denuder samplers (that measure $NH_3$ and $NH_4^+$) has been demonstrated and can be recommended for authorities that wish to better understand the behaviour of $NH_x$ in their jurisdictions. It can be noted that in contrast to $NH_3$, particulate $NH_4^+$ concentrations are spatially rather homogeneous and this may allow for some optimisation of $NH_x$ monitoring networks.

An implication that has not been investigated in this analysis is the impact of an increasing $NH_3/NH_x$ ratio on the import and export of $NH_x$ within and across European countries. For example, the increasing $NH_3/NH_x$ ratio in Switzerland will increase local and regional $NH_3$ deposition around the immediate vicinity of emission sources and will potentially lead to excessive nitrogen deposition due to the flux being greater than the local terrestrial and aquatic ecosystems' critical loading thresholds. Further exacerbating this issue is that $NH_3$ has a far greater dry deposition rate than $NH_4^+$ (Paulot et al., 2013). However, these processes will also have the side effect of reducing $NH_4^+$ formation, reducing secondary PM generation, and therefore may lead to less PM transport and exported nitrogen to neighbouring countries. Investigation into these processes is beyond the scope of this work, but the altering of nitrogen deposition budgets is an important feature for European collaborative efforts such as those contained in EMEP (European monitoring and evaluation programme). The long-term trend of country-to-itself contributions to reduced nitrogen deposition was investigated by Fagerli et al. (2021), where increasing trends have been found for half of the considered European countries including Switzerland. Furthermore, the coupling of the above issues with the increasing temperatures resulting from climate change (Masson-Delmotte et al., 2021), trends of $NH_3$ emissions and concentrations can be expected to increase because the increase of temperatures influences not only emissions but also gas-to-particle conversion rates (Sutton et al., 2013).

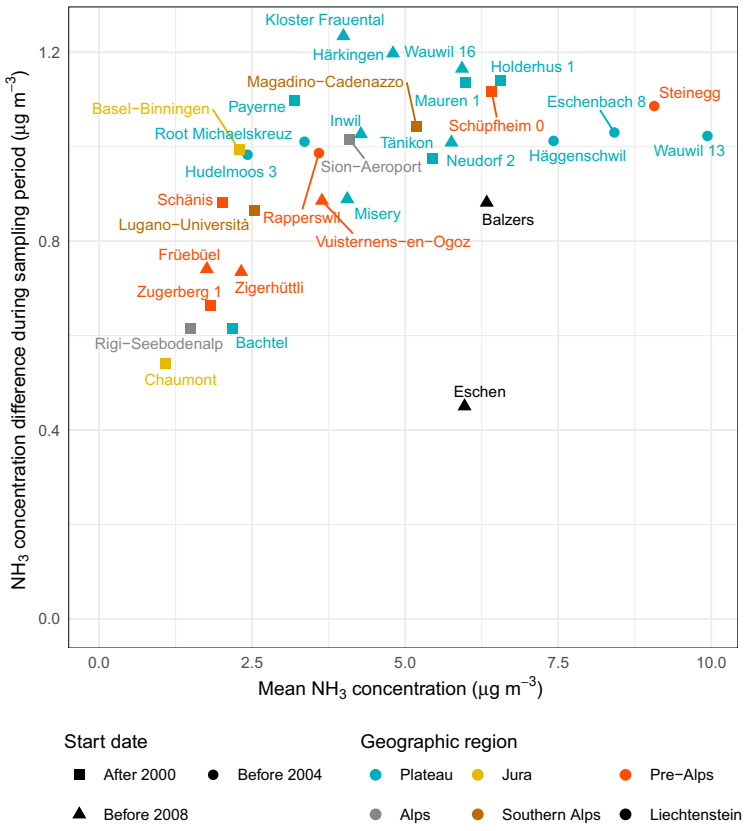


**Fig. A7.** Scatterplot of mean $NH_3$ concentrations (between 2004 and 2021) and the difference of $NH_3$ trend estimates for 32 sampling locations between what was observed and what was simulated using past nitrate ($NO_3^-$) and sulfate ($SO_4^{2-}$) concentrations adjusted for sampling duration.

It seems that reduced nitrogen species will continue to be a problematic group of pollutants throughout Europe, even as the importance of oxidised nitrogen species is poised to become less of an issue over the next couple of decades mostly due to effective vehicular emission control. With the revised World Health Organization's (WHO) global air quality guidelines of 2021 (World Health Organization, 2021) stating very ambitious guideline values for $PM_{10}$ and $PM_{2.5}$, $NH_x$ will continue to be a priority to ensure ambient PM concentrations continue to progress downwards towards the new WHO guideline values. In order to achieve reactive nitrogen deposition fluxes that are below critical load

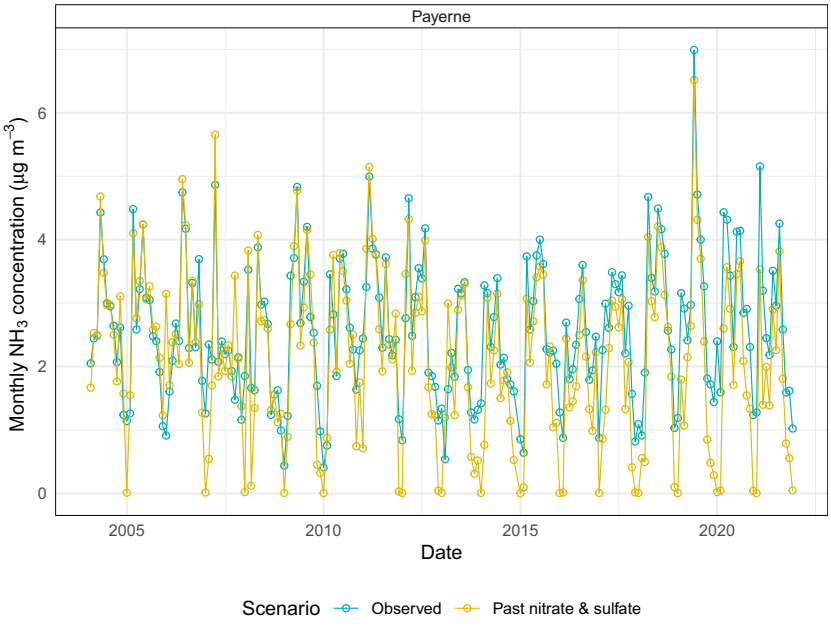


**Fig. A8.** An example of wintertime $NH_3$ depletion at the Payerne sampling location when nitrate ($NO_3^-$) and sulfate ($SO_4^{2-}$) concentrations were fixed at their past (2004–2006) values. Observed $NH_3$ concentrations are shown for comparison.

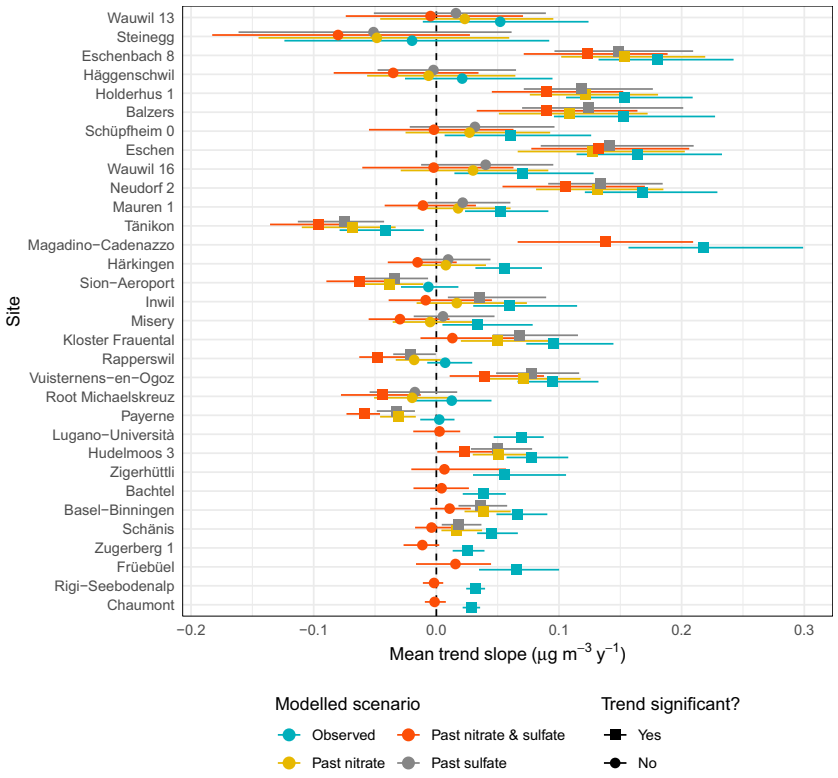


**Fig. A9.** ISORROPIA II-derived $NH_3$ trend slopes for four scenarios between 2004 and 2021 for 32 sampling locations in Switzerland and Liechtenstein. The sites are ordered by their mean $NH_3$ concentration.

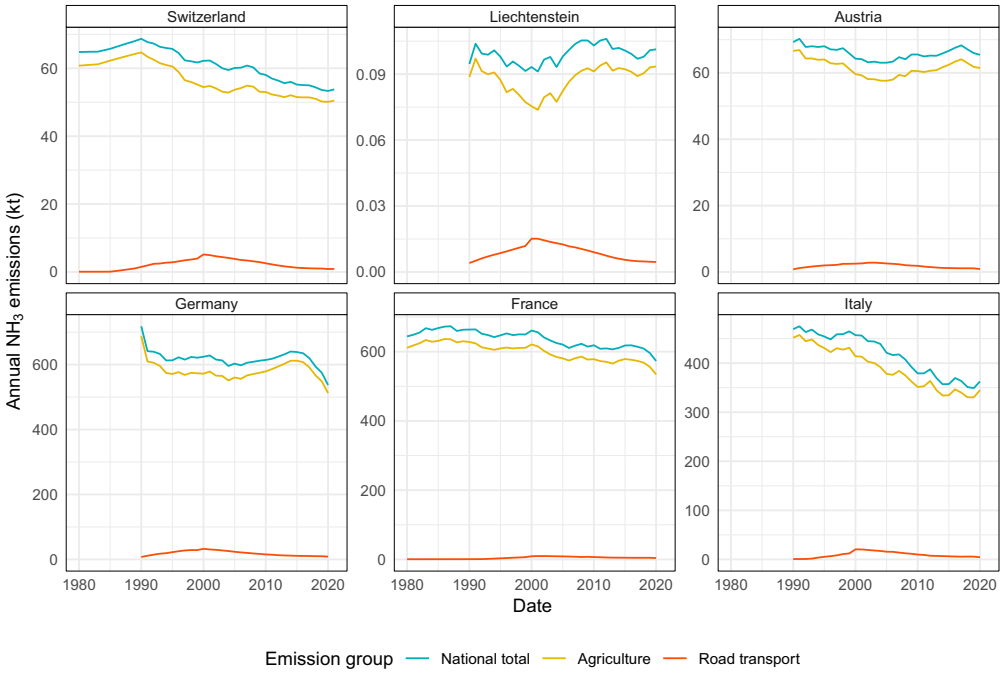


**Fig. A10.** Annual $NH_3$ emissions for three selected sectors for Switzerland, Liechtenstein, and four surrounding countries between 1980 and 2021. Data are from EMEP Centre on Emission Inventories and Projections (2023).

thresholds to avoid further degradation of sensitive and semi-natural ecosystems, substantial $NH_3$ emission reductions are still required.

## CRediT authorship contribution statement

**Stuart K. Grange:** Conceptualization, Methodology, Software, Visualization, Investigation, Writing – original draft. **Jörg Sintermann:** Conceptualization, Methodology, Writing – review & editing. **Christoph Hueglin:** Methodology, Investigation, Writing – original draft.

## Declaration of competing interest

Stuart K. Grange reports financial support was provided by Federal Office for the Environment.

## Data availability

Data will be made available on request.

## Acknowledgements

This work was funded by the Federal Office for the Environment (FOEN) [contract number: 20.0077.PJ/1E5F61F12]. SKG is also supported by
the Natural Environment Research Council (NERC) while holding associate status at the University of York. The authors thank Reto Meier from Air Pollution Control and Chemicals Division, Federal Office for the Environment (FOEN) for their contributions. Lukas Hüglin is thanked the technical assistance when creating the graphical abstract.

## Appendix A. Appendix

## References

Aksoyoglu, S., Jiang, J., Ciarelli, G., Baltensperger, U., Prévôt, A.S.H., 2020. Role of ammonia in European air quality with changing land and ship emissions between 1990 and 2030. Atmos. Chem. Phys. 20, 15665–15680. https://acp.copernicus.org/articles/20/15665/2020/. https://doi.org/10.5194/acp-20-15665-2020.

Alebic-Juretic, A., 2008. Airborne ammonia and ammonium within the northern Adriatic area, Croatia. Environ. Pollut. 154, 439–447. https://www.sciencedirect.com/science/article/pii/S0269749107005921. https://doi.org/10.1016/j.envpol.2007.11.029.

Ansari, A.S., Pandis, S.N., 1998. Response of inorganic PM to precursor concentrations. Environ. Sci. Technol. 32, 2706–2714. https://doi.org/10.1021/es971130j.

Bleeker, A., Sutton, M.A., Acherman, B., Alebic-Juretic, A., Aneja, V.P., Ellermann, T., Erisman, J.W., Fowler, D., Fagerli, H., Gauger, T., Harlen, K.S., Hole, L.R., Horvath, L., Mitosinkova, M., Smith, R.I., Tang, Y.S., van Pul, A., 2009. Linking ammonia emission trends to measured concentrations and deposition of reduced nitrogen at different scales. In: Sutton, M.A., Reis, S., Baker, S.M.H. (Eds.), Atmospheric Ammonia: Detecting Emission Changes and Environmental Impacts. Springer, Netherlands, Dordrecht, pp. 123–180. https://doi.org/10.1007/978-1-4020-9121-6_11.

Bundesamt für Statistik, 2021. Statistischer Atlas der Schweiz – 07 - Land-, Forstwirtschaft / Landwirtschaft / Grossvieheinheiten / 2021 – Grossvieheinheiten 2021. https://www.atlas.bfs.admin.ch/maps/13/de/16763_5896_5872_4801/26099.html.

Bundesamt für Umwelt, . Übermässigkeit von Stickstoff-Einträgen und Ammoniak-Immissionen. https://www.bafu.admin.ch/bafu/de/home/themen/luft/publikationen-studien/publikationen/uebermaessigkeit-von-stickstoff-eintraegen-und-ammoniak-immissionen.html. Bewertung anhand von Critical Loads und Critical Levels insbesondere im Hinblick auf einen kantonalen Massnahmenplan Luftreinhaltung. UV-2003-D, Nummer.

Bundesamt für Umwelt, 2022. Luftqualität 2021 – Messresultate des Nationalen Beobachtungsnetzes für Luftfremdstoffe (NABEL). www.bafu.admin.ch/uz-2227-d. Umwelt-Zustand Nr. 2227: 29 S.

Butler, T., Vermeylen, F., Lehmann, C.M., Likens, G.E., Puchalski, M., 2016. Increasing ammonia concentration trends in large regions of the USA derived from the NADP/AMoN Network 146, 132–140. URL: https://www.sciencedirect.com/science/article/pii/S1352231016304666, doi:https://doi.org/10.1016/j.atmosenv.2016.06.033.

Carslaw, D.C., Ropkins, K., 2012. *openair* — An R package for air quality data analysis. Environ. Model Softw. 27–28, 52–61. http://www.sciencedirect.com/science/article/pii/S1364815211002064.

Copernicus Climate Change Service (C3S), 2017. ERA5: Fifth Generation of ECMWF Atmospheric Reanalyses of the Global Climate. https://doi.org/10.24381/cds.adbb2d47. ERA5 hourly data on single levels from 1979 to present.

Degraeuwe, B., Thunis, P., Clappier, A., Weiss, M., Lefebvre, W., Janssen, S., Vranckx, S., 2017. Impact of passenger car $NO_x$ emissions on urban $NO_2$ pollution - scenario analysis for 8 European cities. Atmos. Environ. 171, 330–337. https://www.sciencedirect.com/science/article/pii/S1352231017307057. https://doi.org/10.1016/j.atmosenv.2017.10.040.

EMEP Centre on Emission Inventories and Projections, 2023. 2023 Submission. https://www.ceip.at/status-of-reporting-and-review-results/2023-submission. Last accessed 2023-03-04.

EMPA, 2020. Technischer Bericht zum Nationalen Beobachtungsnetz für Luftfremdstoffe (NABEL). https://www.bafu.admin.ch/dam/bafu/en/dokumente/luft/fachinfo-daten/technischer_berichtzumnationalenbeobachtungsnetzfuerluftfremdsto.pdf.download.pdf/technischer_berichtzumnationalenbeobachtungsnetzfuerluftfremdsto.pdf. Prepared for BAFU.

European Environment Agency, 2020. Air Quality in Europe – 2020 Report. https://www.eea.europa.eu//publications/air-quality-in-europe-2020-report. EEA Report No 9/2020.

Fagerli, H., Tsyro, S., Simpson, D., Nyíri, A., Wind, P., Gauss, M., Benedictow, A., Klein, H., Valdebenito, A., Mu, Q., Waersted, E.G., Gliß, J., Brenna, H., Mortier, A., Griesfeller, J., Aas, W., Hjellbrekke, A., Solberg, S., Tørseth, K., Yttri, K.E., Mareckova, K., Matthews, B., Schindlbacher, S., Ullrich, B., Wankmüller, R., Scheuschner, T., Kuenen, J.J.P., . Transboundary Particulate Matter, Photo-Oxidants, Acidifying and Eutrophying Components. https://emep.int/publ/reports/2021/EMEP_Status_Report_1_2021.pdf. EMEP Status Report 2021; September 3, 2021.

Federal Office for the Environment, 2020. Production regions NFI. https://www.geocat.ch/geonetwork/srv/eng/md.viewer#/full_view/3cc48f49-5641-4bd9-a5a9-22ab01063147/tab/complete. CH1903+ (LV95).

Federal Office for the Environment, 2021. Switzerland's Informative Inventory Report 2021 (IIR). Submission under the UNECE Convention on Long-range Transboundary Air Pollution. March, 2021.

Federal Office for the Environment, . UNECE-CLRTAP Submission of air pollutant emissions for Switzerland 1980–2020. https://www.ceip.at/status-of-reporting-and-review-results/2022-submission. Deliveries for LRTAP Convention – National emission inventories. 10 Feb 2022.

Federal Office for the Environment, 2022a. Switzerland's Greenhouse Gas Inventory 1990–2020: National Inventory Reportand reporting tables (CRF). Submission of April 2022 under the United Nations Framework Convention on Climate Change and under the Kyoto Protocol. Federal Office for the Environment, Bern. https://www.bafu.admin.ch/bafu/en/home/topics/climate/state/data/climate-reporting/latest-ghg-inventory.html. Submission of April 2022 under the United Nations Framework Convention on Climate Change and under the Kyoto Protocol.

Federal Office for the Environment. Switzerland's Informative Inventory Report 2022 (IIR). Submission under the UNECE Convention on Long-range Transboundary Air Pollution. https://www.bafu.admin.ch/dam/bafu/de/dokumente/luft/fachinfo-daten/switzerlands-informative-rep-2022.pdf.download.pdf/switzerlands-informative-rep-2022.pdf.

Ferm, M., Hellsten, S., 2012. Trends in atmospheric ammonia and particulate ammonium concentrations in Sweden and its causes. Atmos. Environ. 61, 30–39. https://www.sciencedirect.com/science/article/pii/S1352231012006826. https://doi.org/10.1016/j.atmosenv.2012.07.010.

Ferm, M., Svanberg, P.A., 1998. Cost-efficient techniques for urban- and background measurements of $SO_2$ and $NO_2$. Atmos. Environ. 32, 1377–1381. https://www.sciencedirect.com/science/article/pii/S1352231097001702. https://doi.org/10.1016/S1352-2310(97)00170-2.

Finlayson-Pitts, B.J., Pitts, J.N.J., 2000. Chemistry of the Upper and Lower Atmosphere: Theory, Experiments, and Applications. Academic Press, San Diego, California.

Fountoukis, C., Nenes, A., 2007. ISORROPIA II: a computationally efficient thermodynamic equilibrium model for $K^+$-$Ca^{2+}$-$Mg^{2+}$-$NH_4^+$-$Na^+$-$SO_4^{2-}$–$NO_3^-$–$Cl^-$–$H_2O$ aerosols. Atmos. Chem. Phys. 7, 4639–4659. https://www.atmos-chem-phys.net/7/4639/2007/. https://doi.org/10.5194/acp-7-4639-2007.

Frei, J., . Agrarumweltindikatoren (AUI). https://2021.agrarbericht.ch/de/umwelt/agrarumweltmonitoring/agrarumweltindikatoren-aui?highlight=ammoniak. Agricultural Report, 2021. BLW, Fachbereich Agrarumweltsysteme und Nährstoffe.

FUB - Forschungsstelle für Umweltbeobachtung AG, 2022. https://www.fub-ag.ch.

Grange, S.K.. Isorropiar: command the aerosol thermodynamical equilibrium ISORROPIA II model with R. https://github.com/skgrange/isorropiar.

Grange, S.K., 2022b. Resources for Publication "Meteorologically Normalised Long-term Trends of Atmospheric Ammonia ($NH_3$) in Switzerland/Liechtenstein and the Explanatory Role of Gas-aerosol Partitioning" https://doi.org/10.5281/zenodo.7100723.

Grange, S.K., Carslaw, D.C., 2019. Using meteorological normalisation to detect interventions in air quality time series. Sci. Total Environ. 653, 578–588. http://www.sciencedirect.com/science/article/pii/S004896971834244X.

Grange, S.K., Carslaw, D.C., Lewis, A.C., Boleti, E., Hueglin, C., 2018. Random forest meteorological normalisation models for Swiss $PM_{10}$ trend analysis. Atmos. Chem. Phys. 18, 6223–6239. https://acp.copernicus.org/articles/18/6223/2018. https://doi.org/10.5194/acp-18-6223-2018.

Grange, S.K., Fischer, A., Zellweger, C., Alastuey, A., Quero, X., Jaffrezo, J.L., Weber, S., Uzu, G., Hueglin, C., 2021. Switzerland's $PM_{10}$ and $PM_{2.5}$ environmental increments show the importance of non-exhaust emissions. Atmos. Environ. X 12, 100145. https://www.sciencedirect.com/science/article/pii/S2590162121000459. https://doi.org/10.1016/j.aeaoa.2021.100145.

Grange, S.K., Uzu, G., Weber, S., Jaffrezo, J.L., Hueglin, C., 2022. Linking Switzerland's $PM_{10}$ and $PM_{2.5}$ oxidative potential (OP) with emission sources. Atmos. Chem. Phys.

22, 7029–7050. https://acp.copernicus.org/articles/22/7029/2022/. https://doi.org/10.5194/acp-22-7029-2022.
Häni, C., Kupper, T., 2021. Trendanalyse Ammoniak-Konzentrationen Kanton Zürich. Bericht zur Messperiode 2012–2019. Passivsammler Messungen. Im Auftrag des Amts für Abfall, Wasser, Energie und Luft Kanton Zürich.
Hertel, O., Skjøth, C.A., Løfstrøm, P., Geels, C., Frohn, L.M., Ellermann, T., Madsen, P.V., 2006. Modelling nitrogen deposition on a local scale—a review of the current state of the art. Environ. Chem. 3, 317–337. https://doi.org/10.1071/EN06038.
Hüglin, C., Grange, S.K., . Chemical Characterisation and Source Identification of $PM_{10}$ and $PM_{2.5}$ in Switzerland. https://www.bafu.admin.ch/dam/bafu/de/dokumente/luft/externe-studien-berichte/chemical-characterisation-and-source-identification-of-pm-in-switzerland.pdf.download.pdf/Characterisation-source-identification-PM.pdf. Project Report. Empa, Swiss Federal Laboratories for Materials Science and Technology. Commissioned by the Federal Office for the Environment (FOEN).
Jacobsen, B.H., Latacz-Lohmann, U., Luesink, H., Michels, R., Ståhl, L., 2019. Costs of regulating ammonia emissions from livestock farms near Natura 2000 areas - analyses of case farms from Germany, Netherlands and Denmark. J. Environ. Manag. 246, 897–908. https://www.sciencedirect.com/science/article/pii/S0301479719307340. https://doi.org/10.1016/j.jenvman.2019.05.106.
Kupper, T., Bonjour, C., Menzi, H., 2015. Evolution of farm and manure management and their influence on ammonia emissions from agriculture in Switzerland between 1990 and 2010. Atmos. Environ. 103, 215–221. https://www.sciencedirect.com/science/article/pii/S1352231014009728. https://doi.org/10.1016/j.atmosenv.2014.12.024.
Lang, P., 2020. New Approaches to the Statistical Analysis of Air Quality Network Data: Insights from Application to National and Regional UK Networks. Ph.D. thesis. University of York. https://etheses.whiterose.ac.uk/28164/.
Masson-Delmotte, V., Zhai, P., Pirani, A., Connors, S.L., Péan, C., Berger, S., Caud, N., Chen, Y., Goldfarb, L., Gomis, M.I., Huang, M., Leitzell, K., Lonnoy, E., Matthews, J. B.R., Maycock, T.K., Waterfield, T., Yelekçi, O., Yu, R., Zhou, B., 2021. IPCC, 2021: Summary for Policymakers. In: Climate Change 2021: The Physical Science Basis. Contribution of Working Group I to the Sixth Assessment Report of the Intergovernmental Panel on Climate Change. Cambridge University Press. https://www.ipcc.ch/report/ar6/wg1.
Nair, A.A., Yu, F., 2020. Quantification of atmospheric ammonia concentrations: a review of its measurement and modeling. Atmosphere 11, 1092. https://www.mdpi.com/2073-4433/11/10/1092.
Paulot, F., Jacob, D.J., Henze, D.K., 2013. Sources and processes contributing to nitrogen deposition: an adjoint model analysis applied to biodiversity hotspots worldwide. Environ. Sci. Technol. 47, 3226–3233. https://doi.org/10.1021/es3027727.
Philipp, M., Locher, R., . Trendanalyse $NH_3$-Immissionsmessungen in der Schweiz. https://digitalcollection.zhaw.ch/handle/11475/14101. Im Auftrag des Bundesamt für Umwelt (BAFU). https://doi.org/10.21256/zhaw-3440.
Pinder, R.W., Gilliland, A.B., Dennis, R.L., 2008. Environmental impact of atmospheric $NH_3$ emissions under present and future conditions in the eastern United States. Geophys. Res. Lett. 35, 6. https://agupubs.onlinelibrary.wiley.com/doi/abs/10.1029/2008GL033732. https://doi.org/10.1029/2008GL033732.
R Core Team, 2019. R: A Language and Environment for Statistical Computing. https://www.R-project.org/.
Radiello, 2021. The Radial Symmetry Diffusive Sampler. https://radiello.com.
Renner, E., Wolke, R., 2010. Modelling the formation and atmospheric transport of secondary inorganic aerosols with special attention to regions with high ammonia emissions. Atmos. Environ. 44, 1904–1912. https://www.sciencedirect.com/science/article/pii/S1352231010001354. https://doi.org/10.1016/j.atmosenv.2010.02.018.
Schiferl, L.D., Heald, C.L., Van Damme, M., Clarisse, L., Clerbaux, C., Coheur, P.F., Nowak, J.B., Neuman, J.A., Herndon, S.C., Roscioli, J.R., Eilerman, S.J., 2016. Interannual variability of ammonia concentrations over the United States: sources and implications. Atmos. Chem. Phys. 16, 12305–12328. https://acp.copernicus.org/articles/16/12305/2016/. https://doi.org/10.5194/acp-16-12305-2016.
Seitler, E., Meier, M., . Ammoniak-Immissionsmessungen in der Schweiz 2000 bis 2021 Messbericht. https://www.bafu.admin.ch/dam/bafu/de/dokumente/luft/externe-studien-berichte/ammoniak-immissionsmessungen-in-der-schweiz-2000-2021.pdf.download.pdf/Ammoniak-Immissionsmessungen_CH_2000-2021.pdf. FUB - Forschungsstelle für Umweltbeobachtung AG.
Seitler, E., Thöni, L., 2009. Ammoniak-Immissionsmessungen in der Schweiz–Sammel- und Messmethoden.
Sofia, D., Gioiella, F., Lotrecchiano, N., Giuliano, A., 2020. Mitigation strategies for reducing air pollution. Environ. Sci. Pollut. Res. 27, 19226–19235. https://doi.org/10.1007/s11356-020-08647-x.
Sutton, M.A., Asman, W.A.H., Ellermann, T., Van Jaarsveld, J.A., Acker, K., Aneja, V., Duyzer, J., Horvath, L., Paramonov, S., Mitosinkova, M., Tang, Y.S., Achermann, B., Gauger, T., Bartniki, J., Neftel, A., Erisman, J.W., 2003. Establishing the link between ammonia emission control and measurements of reduced nitrogen concentrations and deposition. Environ. Monit. Assess. 82, 149–185. https://doi.org/10.1023/A:1021834132138.
Sutton, M.A., Reis, S., Riddick, S.N., Dragosits, U., Nemitz, E., Theobald, M.R., Tang, Y.S., Braban, C.F., Vieno, M., Dore, A.J., Mitchell, R.F., Wanless, S., Daunt, F., Fowler, D., Blackall, T.D., Milford, C., Flechard, C.R., Loubet, B., Massad, R., Cellier, P., Personne, E., Coheur, P.F., Clarisse, L., Van Damme, M., Ngadi, Y., Clerbaux, C., Skjøth, C.A., Geels, C., Hertel, O., Wichink Kruit, R.J., Pinder, R.W., Bash, J.O., Walker, J.T., Simpson, D., Horváth, L., Misselbrook, T.H., Bleeker, A., Dentener, F., de Vries, W., 2013. Towards a climate-dependent paradigm of ammonia emission and deposition. In: Philosophical Transactions of the Royal Society B: Biological Sciences, 368, p. 20130166. https://doi.org/10.1098/rstb.2013.0166.
Tang, Y.S., Dragosits, U., van Dijk, N., Love, L., Simmons, I., Sutton, M.A., 2009. Assessment of Ammonia and Ammonium Trends and Relationship to Critical Levels in the UK National Ammonia Monitoring Network (NAMN). Springer Netherlands, pp. 187–194. https://doi.org/10.1007/978-1-4020-9121-6_13.
Tang, Y.S., Braban, C.F., Dragosits, U., Dore, A.J., Simmons, I., van Dijk, N., Poskitt, J., Dos Santos Pereira, G., Keenan, P.O., Conolly, C., Vincent, K., Smith, R.I., Heal, M.R., Sutton, M.A., 2018. Drivers for spatial, temporal and long-term trends in atmospheric ammonia and ammonium in the UK. Atmos. Chem. Phys. 18, 705–733. https://acp.copernicus.org/articles/18/705/2018/. https://doi.org/10.5194/acp-18-705-2018.
The Royal Society, 2021. Effects of Net-Zero Policies and Climate Change on Air Quality. https://royalsociety.org/topics-policy/projects/air-quality-climate-change.
Thöni, L., Seitler, E., Blatter, A., Neftel, A., 2003. A passive sampling method to determine ammonia in ambient air. J. Environ. Monit. 5, 96–99. https://doi.org/10.1039/B209356A. https://doi.org/10.1039/B209356A.
Thöni, L., Brang, P., Braun, S., Seitler, E., Rihm, B., 2004. Ammonia monitoring in Switzerland with passive samplers: patterns, determinants and comparison with modelled concentrations. Environ. Monit. Assess. 98, 93–107. https://doi.org/10.1023/B:EMAS.0000038181.99603.6e.
Van Damme, M., Clarisse, L., Franco, B., Sutton, M.A., Erisman, J.W., Wichink Kruit, R., van Zanten, M., Whitburn, S., Hadji-Lazaro, J., Hurtmans, D., Clerbaux, C., Coheur, P.F., 2021. Global, regional and national trends of atmospheric ammonia derived from a decadal (2008-2018) satellite record. Environ. Res. Lett. 16, 055017 https://doi.org/10.1088/1748-9326/abd5e0.
Vestreng, V., Myhre, G., Fagerli, H., Reis, S., Tarrasón, L., 2007. Twenty-five years of continuous Sulphur dioxide emission reduction in Europe. Atmos. Chem. Phys. 7, 3663–3681. https://acp.copernicus.org/articles/7/3663/2007/. https://doi.org/10.5194/acp-7-3663-2007.
Warner, J.X., Dickerson, R.R., Wei, Z., Strow, L.L., Wang, Y., Liang, Q., 2017. Increased atmospheric ammonia over the world's major agricultural areas detected from space. Geophys. Res. Lett. 44, 2875–2884. https://agupubs.onlinelibrary.wiley.com/doi/abs/10.1002/2016GL072305. https://doi.org/10.1002/2016GL072305.
Wichink Kruit, R.J., Aben, J., de Vries, W., Sauter, F., van der Swaluw, E., van Zanten, M. C., van Pul, W.A.J., 2017. Modelling trends in ammonia in the Netherlands over the period 1990–2014. Atmos. Environ. 154, 20–30. https://www.sciencedirect.com/science/article/pii/S1352231017300316. https://doi.org/10.1016/j.atmosenv.2017.01.031.
Wilcox, R.R., 2004. Some results on extensions and modifications of the Theil-Sen regression estimator. Br. J. Math. Stat. Psychol. 57, 265–280. https://onlinelibrary.wiley.com/doi/abs/10.1348/0007110042307230. https://doi.org/10.1348/0007110042307230.
Wood, S.N., 2011. Fast stable restricted maximum likelihood and marginal likelihood estimation of semiparametric generalized linear models. Journal of the Royal Statistical Society: Series B (Statistical Methodology) 73, 3–36. https://doi.org/10.1111/j.1467-9868.2010.00749.x.
World Health Organization, 2021. WHO global air quality guidelines: particulate matter ($PM_{2.5}$ and $PM_{10}$), ozone, nitrogen dioxide, sulfur dioxide and carbon monoxid. World Health Organization, 300 pp. https://apps.who.int/iris/rest/bitstreams/1371692/retrieve.
Yao, X., Zhang, L., 2016. Trends in atmospheric ammonia at urban, rural, and remote sites across North America. Atmos. Chem. Phys. 16, 11465–11475. https://acp.copernicus.org/articles/16/11465/2016/. https://doi.org/10.5194/acp-16-11465-2016.
Yao, X., Zhang, L., 2019. Causes of large increases in atmospheric ammonia in the last decade across North America. ACS Omega 4, 22133–22142. https://doi.org/10.1021/acsomega.9b03284.
Yu, F., Nair, A.A., Luo, G., 2018. Long-term trend of gaseous ammonia over the United States: modeling and comparison with observations. Journal of Geophysical Research: Atmospheres 123, 8315–8325. https://agupubs.onlinelibrary.wiley.com/doi/abs/10.1029/2018JD028412. https://doi.org/10.1029/2018JD028412.
van Zanten, M., Wichink Kruit, R., Hoogerbrugge, R., Van der Swaluw, E., van Pul, W., 2017. Trends in ammonia measurements in the Netherlands over the period 1993–2014. Atmos. Environ. 148, 352–360. https://www.sciencedirect.com/science/article/pii/S1352231016308780. https://doi.org/10.1016/j.atmosenv.2016.11.007.